The Nerve Growth Factor IB-like Receptor Nurr1 (NR4A2) Recruits CoREST Transcription Repressor Complexes to Silence HIV Following Proviral Reactivation in Microglial Cells

Fengchun Ye*, David Alvarez-Carbonell, Kien Nguyen, Saba Valadkhan, Konstantin Leskov, Yoelvis Garcia-Mesa, Sheetal Sreeram, and Jonathan Karn[1]

[1]Department of Molecular Biology and Microbiology. Case Western Reserve University, Cleveland, Ohio, United States of America

*Corresponding author

E-mail: fxy63@case.edu

Key word: HIV, silencing, microglia, Nurr1, CoREST

Running title: Nurr1 mediates HIV latency in microglial cells

ABSTRACT

Human immune deficiency virus (HIV) infection of microglial cells in the brain leads to chronic neuroinflammation, which is antecedent to the development of HIV-associated neurocognitive disorders (HAND) in the majority of patients. Productively HIV infected microglia release multiple neurotoxins including proinflammatory cytokines and HIV proteins such as envelope glycoprotein (gp120) and transactivator of transcription (Tat). However, powerful counteracting silencing mechanisms in microglial cells result in the rapid shutdown of HIV expression to limit neuronal damage. Here we investigated whether the Nerve Growth Factor IB-like nuclear receptor Nurr1 (NR4A2), which is a repressor of inflammation in the brain, acts to directly restrict HIV expression. HIV silencing was substantially enhanced by Nurr1 agonists in both immortalized human microglial cells (hμglia) and induced pluripotent stem cells (iPSC)-derived human microglial cells (iMG). Overexpression of Nurr1 led to viral suppression, whereas by contrast, knock down (KD) of endogenous Nurr1 blocked HIV silencing. Chromatin immunoprecipitation (ChIP) assays showed that Nurr1 mediates recruitment of the CoREST/HDAC1/G9a/EZH2 transcription repressor complex to HIV promoter resulting in epigenetic silencing of active HIV. Transcriptomic studies demonstrated that in addition to repressing HIV transcription, Nurr1 also downregulated numerous cellular genes involved in inflammation, cell cycle, and metabolism, thus promoting HIV latency and microglial homoeostasis. Thus, Nurr1 plays a pivotal role in modulating the cycles of proviral reactivation by cytokines and potentiating the proviral transcriptional shutdown. These data highlight the therapeutic potential of Nurr1 agonists for inducing HIV silencing

and microglial homeostasis and amelioration of the neuroinflammation associated with HAND.

AUTHOR SUMMARY

HIV enters the brain almost immediately after infection where it infects perivascular macrophages, microglia and, to a less extent, astrocytes. In previous work using an immortalized human microglial cell model, we observed that integrated HIV constantly underwent cycles of reactivation and subsequent silencing. In the present study, we found that the Nurr1 nuclear receptor is a key mediator of HIV silencing. The functional activation of Nurr1 by specific agonists, or the over expression of Nurr1, resulted in rapid silencing of activated HIV in microglial cells. Global gene expression analysis confirmed that Nurr1 not only repressed HIV expression but also regulated numerous genes involved in microglial homeostasis and inflammation. Thus, Nurr1 is pivotal for HIV silencing and repression of inflammation in the brain and is a promising therapeutic target for treatment of HAND.

INTRODUCTION

Human immune deficiency virus (HIV) invades the brain soon after primary infection [1]. The virus infects astrocytes, perivascular macrophages, and microglial cells, but not neurons [2, 3]. However, because microglial cells are much longer-lived than astrocytes and perivascular macrophages and can support productive HIV replication, they are mostly likely to be the main cellular reservoir of HIV in the brain [4, 5]. In later stages of HIV infection, many infected patients develop HIV-associated neurocognitive disorders (HAND) [6]. Although combination antiretroviral therapy (cART) dramatically lowers the levels of HIV RNA in the brain [7, 8], it does not reduce the incidence of HAND [9, 10]. Initial studies indicated, paradoxically, that HAND did not correlate with the number of HIV-infected cells or viral antigens in the central nervous system (CNS) [11, 12], but instead correlates strongly with systemic inflammation and CNS inflammation [13]. However, the early studies neglected both the side effects of anti-HIV drugs on neuronal damage, which could mask the benefits of reduced HIV expression by cART and the impact of HIV latency on the development of HAND.

Over the past decade, the intimate relationship between neuroinflammation, neurodegeneration and abnormal activation of microglial cells has been implicated in a wide range of diverse neurological diseases [14-19]. There are compelling reasons to believe that the physiology of microglia also plays a critical role in the development of HAND. Infected macrophages/microglia in the CNS serve as long-lived cellular reservoirs of HIV-1, even in well-suppressed patients receiving ART [20]. Microglia constitute the first barrier of the innate immune response in the brain and become activated and polarized to maintain the integrity of the CNS [21, 22]. In the normal CNS environment,

healthy neurons provide signals to microglia via secreted and membrane bound factors such as CX3CL1 and neurotransmitters that induce HIV-silencing. By contrast, damaged neurons not only cause activation of the microglia but also induce HIV reactivation [23].

Activated microglia secrete exaggerated amounts of neurotoxins such as tumor necrosis factor-alpha (TNF-α), nitric oxide, interleukin-6 (IL-6), interleukin-1 beta (IL-1β), reactive free radicals, and matrix metallopeptidases (MMPs) [24, 25]. The production of these cytotoxic factors is augmented by HIV infection [23, 26]. Mounting evidence indicates that HIV proteins such as transactivator of transcription (Tat), negative regulatory factor (Nef), envelope glycoprotein gp120, and viral RNA are not only directly neurotoxic, but also contribute to inflammation in the brain by activating microglial cells [27-35]. On the other hand, some of the inflammatory cytokines such as TNF-α strongly induce HIV expression in microglial cells through autocrine signaling, creating cycles of HIV reactivation and chronic inflammation in the brain [36]. It is therefore important to determine the factors responsible for inducing HIV reactivation and inflammation and explore cellular mechanisms that antagonize these factors in order to develop treatment for HAND.

A major constraint for studying HIV infection and replication in the brain is the difficulty of obtaining native microglial cells from brain biopsies. We therefore developed a microglial cell model by immortalizing human primary microglial cells with the simian virus large T-antigen (SV40) and the human telomerase reverse transcriptase (hTERT) [37]. The immortalized microglia retain the typical structure and morphology of primary microglial cells, express microglial cell markers, and display microglial cell activities such as migration and phagocytosis [37].

A unique feature of HIV infection of microglial cells is that the virus is able to quickly establish latency [23, 36-38]. In microglial cells, transcription initiation is primarily regulated by NF-κB. In resting microglia (M0 stage), NF-κB is sequestered in the cytoplasm [23, 36-38]. However, unlike memory T-cells, P-TEFb is not disrupted, although it is inhibited by CTIP2 [39, 40]. The provirus is also silenced epigenetically through the CoREST and polycomb repressive complex 2 (PRC2) histone methyltransferase machinery [4, 41-44]. Activation of microglia by pro-inflammatory signals, such as TNF-α, reversed these molecular restrictions and leads to the reactivation of dormant proviruses and neuropathology.

In contrast to T cells where integrated HIV eventually establishes permanent latency until it is activated by cellular signaling events, HIV in microglial cells undergoes cycles of spontaneous reactivation and subsequent silencing [36]. For example, using a co-culture of (iPSC)-derived human microglial cells (iMG) that were infected with HIV and neurons, we demonstrated that HIV expression in iMG was repressed when co-cultured with healthy neurons but induced when co-cultured with damaged neurons [23]. The dynamics of spontaneous reactivation of latent HIV and subsequent silencing of active HIV constantly typically generates two populations in culture: the GFP^- population with transient latent HIV, and the GFP^+ population undergoing active HIV transcription. Spontaneous HIV reactivation in microglial cells could be attenuated by activation of the glucocorticoid receptor (GR) with its ligand dexamethasone (DEXA) [45], which blocked recruitment of NF-κB and AP-1 for HIV transactivation [36, 45]. However, since we consistently observed spontaneous reactivation of latent HIV and subsequent silencing of the active HIV in the absence of dexamethasone, and in co-cultures with neurons, we

126 reasoned that there exist other cellular factors that promote HIV silencing in microglial
127 cells.

128 In the present study, we examined whether three members of the Nerve Growth
129 Factor IB-like nuclear receptor family, which includes nuclear receptor 77 (Nur77,
130 NR4A1), nuclear receptor related 1 (Nurr1, NR4A2), and neuron-derived receptor 1
131 (Nor1, NR4A3), contribute to HIV silencing in microglial cells. These receptors play
132 complementary roles in neurons and microglia to limit inflammatory responses. In
133 neurons, these receptors act as positive transcriptional regulators that control expression
134 of dopamine transporter and tyrosine hydroxylase for differentiation of dopamine neuron,
135 as well as other key genes involved in neuronal survival and brain development [46-49].
136 By contrast, these nuclear receptors can also act as negative transcriptional regulators in
137 microglia cells and suppress expression of inflammatory cytokines such as TNF-α and
138 IL-1β [50]. Because of these combined mechanisms, Nerve Growth Factor IB-like nuclear
139 receptors play a critical role in protection of the brain during neurodegenerative diseases
140 such as Parkinson's disease and Alzheimer's disease [51-56].

141 Here we report that Nurr1 plays a pivotal role in silencing active HIV in microglial
142 cells by recruiting the CoREST/HDAC1/G9a/EZH2 transcription repressor complex to HIV
143 promoter. Our data also demonstrate that Nurr1 promotes microglial homoeostasis and
144 suppression of inflammation in the brain.
145

RESULTS

Nurr1 agonists strongly induce HIV silencing in microglial cells

To study the role of nuclear receptors in the control of HIV expression in the microglia, we used our immortalized human microglial (hμglia) cells [37], which were infected with a recombinant HIV-1 reporter that carried an EGFP marker for "real-time" monitoring of HIV latency and reactivation (**Fig 1A**). One representative clone, HC69 [37, 45], was used for all experiments described in this study. Under normal culture conditions, most cells were GFP-negative (GFP^-) (**Fig 1B** & **C**). Exposure of HC69 cells to TNF-α (400 pg/ml) for 24 hours (hr), induced GFP expression (GFP^+) in over 90% of the cells, demonstrating that majority of the integrated HIV provirus was in a latent state under normal culture conditions. To examine whether the reactivated HIV could revert to latency, we conducted a chase experiment by culturing the activated HC69 cells for 96 hr in fresh medium following TNF-α stimulation for 24 hr and washing with PBS. Notably, the numbers of GFP+ cells decreased from 93.1% to 61.4% at the end of the chase experiment, suggesting the existence of an intrinsic cellular mechanism that silences the activated HIV. This substantial decrease of GFP+ expression was unlikely to be caused by GR-mediated HIV silencing [45], because the cells were cultured in the absence of GR ligand glucocorticoid or dexamethasone.

To understand the regulatory mechanisms of HIV expression in microglial cells, we had previously undertaken a global screening for HIV silencing cellular factors [57, 58] by using a HIV-infected rat microglial cell model (CHME cells) [37, 59]. The latently infected CHME/HIV cells were superinfected with lentiviral vectors carrying a synthetic shRNA library from Cellecta Inc. (Mountain View, CA) containing a total of 82,500

shRNAs targeting 15,439 mRNA sequences [60-62].. Cells carrying reactivated proviruses were then purified by sorting and the shRNA sequences were identified by next-generation sequencing and classified by Ingenuity Pathway Analysis (QIAGEN). This powerful new technology, which we have also applied to the identification of latency factors in T-cells and TB-infected myeloid cells [58, 63], has revealed a wide range of factors and pathways critical for maintaining proviral latency in microglial cells. Analysis of the top 25 % "hits" led to our unexpected discovery that members of the nuclear receptors (NRs) families including Thyroid Hormone Receptor-like family members PPARα, PPARβ, PPARγ, and RARβ ranked in the top 5%, the Retinoid X Receptor-like family members RXRα and RXRβ together with the glucocorticoid receptor (GR, NR3C) ranked in the top 15%, and the Nerve Growth Factor IB-like family members NR4A1 (Nur77), NR4A2 (Nurr1) and NR4A3 (Nor1) ranked in the top 25%.

Agonists of the NR4A nuclear receptor family (Nur77 (NR4A1), Nurr1 (NR4A2), and Nor1 (NR4A3)) have been shown to ameliorate neuron degeneration in animal models [53, 64-67]. To confirm a role for the nuclear receptors in HIV silencing, we first treated spontaneously activated HC69 cells with the Nurr1 agonist 6-mercaptopurine (6-MP) [68, 69]. As shown in **Fig 2A**, the frequency of GFP^+ cells decreased in a 6-MP dose-dependent manner. Data from Western blot analysis showed that HC69 cells constitutively expressed Nurr1, as well as a very low level of Nor1 (**Fig 2B**), but Nur77 expression in these cells was below the detection limit. Treatment with 6-MP slightly increased expression of Nurr1. Expression of HIV, as measured by the levels of Nef protein, was strongly inhibited in a dose-dependent manner. Notably, as a control for the role of Nurr1 in cellular gene expression, 6-MP also substantially reduced expression of

MMP2, which is a well-known repression target of Nurr1 and a neurotoxin involved in the development of HAND [70, 71].

In addition, the Retinoid X Receptor-like family members also play a critical role in silencing inflammation in the brain [72, 73]. We also screened various agonists of the nuclear receptors for their effect on HIV expression in HC69 microglia (**Fig 2C**). We induced maximum HIV expression in HC69 cells with high dose (400 pg/ml) TNF-α for 24 hr, followed by a chase experiment during which the induced cells were cultured in the absence or presence of various agonists, alone or in combination. Consistent with our previous gene manipulation data, the RXRα/β/γ agonist bexarotene (BEX) [74-77] silenced HIV expression on its own, although it was less potent than 6-MP. Interestingly, combinations of 6-MP with DEXA and BEX displayed additive HIV silencing effects, suggesting that they each had distinct mechanisms of action.

Nurr1 overexpression enhances HIV silencing

To further examine how the nuclear receptors contribute to HIV silencing, we constructed lentiviral vectors expressing N-terminal 3X-FLAG-tagged Nur77, Nurr1, and Nor1 respectively under the control of a CMV promoter. Infection of HC69 cells with the different lentiviruses generated cell lines that stably expressed FLAG-tagged Nur77, Nurr1, Nor1, and empty vector, respectively, as confirmed by RNA-Seq studies (**Fig 3A**) western blots (**Fig 3B**).

To examine how overexpression of each of these nuclear receptors modulated HIV proviral activation and silencing, we stimulated all four cell lines with high dose (400 pg/ml) TNF-α for 24 hr to induce HIV transcription through activation of NF-κB [38], followed by a 48 hr chase experiment in which TNF-α was removed by washing the cells with PBS

followed by the addition of media lacking TNF-α (**Fig 3C**). As shown by western blot in **Fig 3D**, TNF-α strongly induced the expression of HIV Nef protein, which we used as a marker of HIV reactivation, in all cell lines at 24 hr. Notably, Nef expression decreased in all four cell lines 48 hr after TNF-α withdrawal. However, the reduction in Nef expression was much more pronounced in HC69 cells that express 3X-FLAG-Nurr1, suggesting that overexpression of Nurr1 enhanced silencing of active HIV in HC69 cells.

We rigorously confirmed these findings using the RNA-Seq data (**Fig 3E**) to measure the fluctuations in both HIV and Nurr1 expression. In the Nurr1 overexpressing cells, even in unstimulated conditions, the level of HIV proviral expression was strongly reduced. Following stimulation with either a low dose (20 pg/ml) or high dose (400 pg/ml) TNF-α, both vector-infected and Nurr1 overexpressing cells showed an increase in proviral expression. While the level of HIV expression was similar between control cells (vector-infected) and Nurr1-overexpressing cells after high dose TNF-α stimulation, Nurr1 overexpressing cells had much lower proviral expression level after low dose TNF-α stimulation (**Fig 3E**). The level of HIV mRNA after withdrawal of high dose TNF-α was three times lower in Nurr1 overexpressing cells than in vector-infected cells (**Fig 3E**), strongly suggesting that overexpression of Nurr1 enhanced silencing of active HIV in HC69 cells.

Nurr1 knockdown blocks HIV silencing

As a complementary approach we performed shRNA-mediated knock down (KD) of endogenous Nurr1 in HC69 cells. Cell lines that stably expressed Nurr1-specific or control shRNA were verified for effective Nurr1 KD by RNA-Seq analyses (**Fig 4A**) Following the protocol described in **Fig 4B**, control and KD cells were activated with a

high dose (400 pg/ml) TNF-α for 24 hr, followed by a 72 hr chase. Western blot analyses confirmed the Nurr1 knock down efficiency (**Fig 4C**). The blots also showed that HIV Nef protein, which is a measure of HIV transcription, was strongly induced at 24 hr post TNF-α stimulation in both the control and the Nurr1 KD cells. However, after the chase, Nef levels decreased significantly in the control cells but remained high in Nurr1 KD cells (**Fig 4C**).

Similar results were obtained using flow cytometry (**Fig 4D**). Compared to cells expressing control shRNA with 10.5% GFP+ cells, the Nurr1 KD cells displayed 58.8% GFP^+ cells even before TNF-α stimulation, which most likely resulted from failure of silencing spontaneously reactivated HIV in these cells due to Nurr1 depletion (**Fig 4D**). As expected, after exposure to high dose TNF-α for 24 hr, both the control and Nurr1 KD cell lines expressed equally high levels of GFP expression (**Fig 4D**), displaying 86.3% and 91.2% GFP+ cells respectively. However, 72 hrs after TNF-α withdrawal, GFP expression decreased significantly in cells expressing the control shRNA (47.2% GFP+) but remained high (74.6% GFP+) in the Nurr1 KD cells (**Fig 4D**). Finally, the overall mRNA level of the HIV measured by RNA-Seq was about 1.7 times higher in Nurr1 KD at the end of the chase experiment (**Fig 4E**).

Thus, both the overexpression and the reciprocal KD experiments confirmed an essential role of Nurr1 in the silencing HIV in microglial cells.

Nurr1 drives activated microglial cells towards homeostasis

Our RNA-Seq data also provided important insights into the cellular pathways that were impacted by Nurr-1 over- and under-expression. We focused our attention on the changes in cellular transcriptome during the chase step following TNF-α induction since, as described above, this is the stage where Nurr1 has the greatest impact on HIV gene

expression. As shown by the differential gene expression curves in **Fig 5A,** a small subset of genes are selectively up and down regulated during the chase. A larger number of genes were differentially expressed in Nurr1 overexpressing cells compared to control cells (**Fig 5A & S1 Fig.**). Pathways that showed the most statistically significant changes in response to Nurr1 overexpression included the downregulation of key pathways with critical roles in cellular proliferation and metabolism including: MYC, E2F and MTORC signaling and G2M checkpoint (**Fig 5B**). By contrast, KD of Nurr1 by shRNA did not selectively activate any major signaling pathways.

It is important to note that Nurr1 overexpression did not significantly interfere with the TNF-α signaling pathway during any step of these experiments (**Fig 5B**), suggesting that the cellular proliferation pathways we have identified are directly regulated by Nurr1. To further address this issue and determine whether Nurr1 simply accelerated the reversal of the normal microglial response to TNF-α stimulation during the chase, or if it regulated a distinct set of genes and pathways, we performed a gene trajectory analysis (**Fig 6A, S2 Fig**).

For the trajectory analysis we included RNA-Seq data from cells that were treated with the low dose of TNF-α (20 pg/ml), to simulate a sub-optimal activation signal. A pseudo-trajectory was defined containing three steps: Step 1 defines the changes in gene expression following stimulation with low dose TNF-α compared to untreated cells. Step 2 defines additional changes after stimulation with high dose TNF-α compared to cells treated with low dose TNF-α. Step 3 defines the gene expression changes following the chase step compared to cells treated with high dose TNF-α (**S2 Fig**). For each of these steps we calculated whether the expressed protein-coding genes were either upregulated

(designated as “u”), downregulated (designated as “d”) or did not show differential expression in a statistically significant manner (designated as “n”). Genes that showed similar patterns of changes during each step were placed in the same category and named according to their pattern of change during these treatment steps. For example, those that did not show a change after low dose TNF-α stimulation (thus marked as n for Step 1), but were downregulated after high dose TNF-α treatment compared to cells treated with low dose TNF-α (marked as d for Step 2), and showed upregulation during the chase study compared to cells treated with high dose TNF-α (marked as u for step 3), were therefore designated as ndu.

Most genes did not show any change in their expression following the above treatments (designated as the “nnn” group) in both control (vector) and Nurr1-overexpressing cells (**Fig 6A**, **S2 Fig**), and as expected, control cells had higher numbers of nnn group genes than Nurr1 overexpressing cells.

Among those genes that showed an expression change in Nurr1 overexpressing cells, the majority belonged to genes that were not differentially expressed after either a low or high dose TNF-α treatment and exclusively changed their expression profiles during the chase step (i.e., nnu and nnd trajectories, **Fig 6A**, **S2 Fig**). We also noted that the number of genes in these two trajectories were markedly higher in Nurr1 overexpressing cells compared to control cells (i.e., over 800 and 1400 genes for nnu and nnd trajectories, respectively) while the number of genes in other trajectories with the exception of nnn differed by less than 100 genes (**Fig 6A**, **S2 Fig**).

We next confirmed that the genes showing the nnu and nnd trajectories in Nurr1 overexpressing cells were derived from a subset of the nnn trajectory genes in the control

group and were therefore exclusively altered during the chase step in Nurr1 overexpressing cells. To further characterize the Nurr1-specific changes in expression patterns, we used the list of genes in each of the trajectories identified in Nurr1 overexpressing cells and defined their trajectory in control cells (**S3 Fig**). This analysis showed that over 1400 and ~800 of the genes that fall into the nnd or nnu trajectories in Nurr1 overexpressing cells, respectively, have the nnn trajectory in control cells (**S3 Fig**). Thus, the main transcriptomic outcome of Nurr1 overexpression compared to control cells is the induction of changes in expression of a group of genes exclusively during the chase step. Importantly, this group of genes are not differentially expressed in the control cells during either of the three steps of these studies, nor during the TNF-α stimulation steps in Nurr1 overexpressing cells and therefore, the action of Nurr1 during the chase step does not correspond to a reversal of the TNF-α-induced changes.

In order to define the functional impact of this Nurr1-specific set of genes, we performed pathway analysis on the subset of genes that had either nnu or nnd trajectories in Nurr1 overexpressing cells, and a nnn trajectory in control cells (**Fig 6B**). Strikingly, these Nurr1-induced changes in gene expression during the chase step once again highlighted the downregulation of several key proliferative pathways, including: MYC, E2F and MTORC signaling, G2M checkpoint regulation, metabolic pathways such as oxidative phosphorylation, and inflammatory pathways such as IFN-α and IFN-γ response pathways (**Fig 6B**).

Heat maps of the differentially expressed genes further emphasized that the vast majority of genes in each pathway were downregulated in Nurr1 overexpressing cells. For example, among 69 and 60 represented MYC and E2F target genes, 66 and 54 were

downregulated in Nurr1 overexpressing cells, respectively (**S4 Fig**). Finally, another compelling way of visualizing these results is to apply the pattern of expression of the Nurr1-specific genes to the KEGG cell cycle pathway (**S5 Fig**). The strong downregulation by Nurr1 at multiple steps in the cell cycle control pathway is immediately obvious.

Finally, we note as another measure of the specificity of the Nurr1 pathway, that the most enriched transcription factor binding motifs in proximity of the promoters of differentially expressed genes following TNF-α stimulation all display promoter motifs consistent with TNF-α activation (**S6 Fig)**.

Thus, the main impact of Nurr1 on the overall cellular response to inflammatory cytokines, in this case TNF-α, was to accelerate the cellular return to homeostasis by shutting down pathways involved in inflammation and microglial activation. While these anti-inflammatory, pro-homeostasis effects could indirectly lead to HIV proviral transcriptional shutdown, the enhanced downregulation of HIV expression in Nurr1 overexpressing cells, even under basal untreated conditions (**Fig 3D**), suggests that in addition to its pro-homeostasis effects, Nurr1 may also directly regulate the expression of the HIV provirus.

Nurr1 promotes the recruitment of the CoREST/HDAC1/G9a/EZH2 repressor complex to the HIV promoter

Previous studies demonstrated that Nurr1 interacted with the corepressor 1 of REST (CoREST) repressor complex [50, 78]. The CoREST complex is comprised of multiple components including CoREST, repressor element-1 silencing transcription factor (REST), HDAC1/2, euchromatic histone lysine N-methyltransferase 2 (EHMT2), also known as *G9a*, lysine (K)-specific demethylase 1A (KDM1A), and enhancer of zeste

2 polycomb repressive complex 2 subunit (EZH2) [79, 80]. In microglial cells and astrocytes, after stimulation with lipopolysaccharide (LPS), Nurr1 promoted recruitment of this complex to the promoters of inflammatory genes such as IL-1β leading to epigenetic silencing. We postulated that the Nurr1/CoREST repression pathway might therefore also lead to direct regulation of HIV silencing as illustrated in **Fig 7A**.

To test this hypothesis, we first conducted co-immunoprecipitation (Co-IP) assays to confirm the association of Nurr1 with the CoREST repressor complex in HC69 cells (**S7 Fig.**). HC69-3X-FLAG-vector and HC69-3X-FLAG-Nurr1 cells were treated with and without a high dose of TNF-α for 4 hr (400 pg/ml) or 24 hr. After 24 hr TNF-α treatment the cells were chased in the absence of TNF-α for a further 24 hr. Total protein lysates from the differently treated cells were immunoprecipitated using a mouse monoclonal anti-FLAG antibody conjugated to magnetic beads. The anti-FLAG beads pulled down not only FLAG-tagged Nurr1 but also CoREST, HDAC1, G9a, and EZH2 from the HC69-3X-FLAG-Nurr1 cell lysates, demonstrating that in the microglial cells Nurr1 bound directly to the CoREST repressor complex. Notably, the amount of CoREST associated with Nurr1 increased after the cells were stimulated with TNF-α. In contrast, the amounts of G9a and EZH2 proteins associated with Nurr1 decreased at 4 hr post-TNF-α stimulation but rebounded at 24 hr post-TNF-α stimulation. Together, these results suggested that the Nurr1/CoREST/HDAC1/G9a/EZH2 complex were most likely dissociated from each other during early time points of TNF-α stimulation but were reassembled at later time points.

We next conducted ChIP-Seq experiments to demonstrate recruitment of the CoREST repressor complex to the activated HIV promoter in microglial cells. As shown

in **Fig 7B,** CoREST, HDAC1, G9a, and EZH2 were all detected on the HIV provirus and were enriched near the promoter region following TNF-α activation. However, the recruitment kinetics of each component was distinct, with CoREST being recruited to HIV promoter during early time points of TNF-α exposure and HDAC1, G9a, and EZH2 being recruited at late time points. These results are consistent with the Co-IP results shown in **S7 Fig**. Specifically, the levels of CoREST at the HIV promoter peaked at 4 hr post-TNF-α stimulation and decreased at 24 hr post-treatment, whereas the levels of G9a, EZH2, and HDAC1 at the HIV promoter decreased at 4 hr post-TNF-α stimulation when compared to un-treated cells. However, these epigenetic silencers returned to HIV promoter in a much more robust manner at 24 hr post-stimulation.

To provide direct evidence that Nurr1 mediates the recruitment of the CoREST/HDAC1/G9a/EZH2 complex to HIV promoter, we treated HC69 cells expressing control shRNA and Nurr1 shRNA with high dose TNF-α, followed by a 24 hr chase. We then conducted additional ChIP experiments and measured the ChIP products by quantitative PCR (qPCR). As shown in **Fig 7C**, CoREST was strongly recruited to HIV promoter at 4 hr post TNF-α stimulation in HC69 cells expressing control shRNA, however, its recruitment was substantially inhibited in Nurr1 KD cells. Similarly, G9a level in HIV promoter peaked at 24 hr post TNF-α stimulation in HC69 cells expressing control shRNA but its recruitment was also reduced in Nurr1 KD cells. Taken together, these results clearly demonstrated a pivotal role for Nurr1 in mediating recruitment of the CoREST/HDAC1/G9a/EZH2 repressor complex to the promoter of active HIV for epigenetic silencing consistent with the model shown in **Fig 7A**.

The CoREST/HDAC1/G9a/EZH2 repressor complex silences HIV in microglial cells

To further investigate how the CoREST/HDAC1/G9a/EZH2 complex contributes to HIV silencing, we treated HC69 cells with high dose (400 pg/ml) TNF-α for 24 hr followed by a chase in the absence or presence of epigenetic inhibitors that target the CoREST complex, specifically: HDAC inhibitor suberoylanilide hydroxamic acid (SAHA), G9a inhibitor UNC0638, and EZH2 inhibitor GSK343. The numbers of GFP+ cells dropped from 88.4% to 67.03% at 48 hr after TNF-α withdrawal when cells were cultured in the absence of the inhibitors (**Fig 8A**). However, in the presence of SAHA, UNC0638, or GSK343, the numbers of GFP+ cells remained higher (i.e., 77.8%, 85.5%, and 84.7% respectively), indicating that functional inhibition of these epigenetic silencers prevented active HIV from reverting to latency.

To confirm the role of these epigenetic silencers, we generated HC69 cell lines stably expressing CoREST-specific shRNA or CRISPR/Cas9/guide RNA (gRNA) for G9a or EZH2. We confirmed successful KD or knock out (KO) of these proteins in these cell lines by Western blot analysis (**Fig 8B** & **C**). The genetically modified cells were activated with a high dose of TNF-α (400 pg/ml) for 24 hr, followed by culturing the cells in the absence of TNF-α for 48 hr and measurement of GFP expression. CoREST KD substantially increased GFP expression (80.1% GFP+ vs. 25.8% in control cell) even without TNF-α stimulation (**Fig 8D**). Stimulation with high-dose TNF-α for 24 hr resulted in 94.1% and 84.9% GFP+ cells in CoREST KD and control cells respectively. However, after TNF-α withdrawal and subsequent culture for 48 h, the numbers of GFP^+ cells decreased significantly in cells expressing control shRNA (67.7%) but remained high in CoREST KD cells (91.3%), confirming that CoREST was crucial for the silencing of active

421 HIV in microglial cells. Similar results were also seen with the G9a and EZH2 KO cell
422 lines (**Fig 8E**).

423 Therefore, both the ChIP experiments and gene knockout results demonstrate a
424 pivotal role for the CoREST/HDAC1/G9a/EZH2 transcription repressor complex in
425 silencing active HIV in microglial cells.

426 **Nurr1 regulates HIV in iPSC-derived microglial cells**

427 Finally, to confirm that Nurr1 is also critical for the silencing of HIV in primary
428 microglial cells, we infected iPSC-derived human microglial cells (iMG) with the same HIV
429 reporter virus described earlier (**Fig 1A)**. About 50% of the iMG became GFP+ two days
430 after HIV infection (**Fig 9A**). We then treated the infected iMG with 6-MP and another
431 Nurr1 agonist, amodiaquine (AQ) [56, 67], for four days. Both 6-MP and AQ decreased
432 the number of GFP+ cells in a dose-dependent manner (**Fig 9B & C)** and lowered the
433 levels of HIV un-spliced transcripts (**Fig 9D**). Both agonists also dose-dependently
434 reduced MMP2 mRNA in iMG (**Fig 9E**). Collectively, results from both hμglia and iMG
435 strongly suggested an important role for Nurr1 in HIV silencing in microglial cells.

436

DISCUSSION

Epigenetic control of HIV latency in microglial cells

Microglial cells are one of the major cellular reservoirs of HIV in the central nervous system (CNS) [4, 5]. These long-lived cells contribute to increased neuroinflammation and oxidative stress [4, 81], and development of HAND by secreting a variety of neurotoxins as well as harmful HIV proteins such as gP120, Tat, Rev, etc. [82, 83]. Eradication or complete silencing of HIV-infected microglial cells is therefore crucial not only for an HIV cure, but also to prevent the development of HAND, which affects the majority of HIV infected individuals.

Previous studies involving HIV-1 infection of transformed cell lines suggested that epigenetic regulation plays a major role in the establishment and persistence of HIV latency in astrocytes and microglial cells [84, 85]. The cellular COUP transcription factor (COUP-TF) interacting protein (CTIP2) forms a large transcriptional repressor complex with epigenetic silences including the histone deacetylases HDAC1/2, the histone methyltransferases SUV39H1 and SET1, the lysine(K)-specific demethylase KDM1, and heterochromatin protein1 (HP1) [86, 87]. Recruitment of this complex to HIV-1 promoter leads to proviral genome silencing due to reduced histone acetylation and increased levels of histone 3 tri-methylations at lysine 9 (H3K9me3) [86-89]. At the same time, CTIP2 forms another complex with CDK9, Cyclin T1, HEXIM1, 7SK snRNA, and high mobility group AT-hook 1 (HMGA1), which is also recruited to HIV-1 promoter [87, 89]. In the absence of HIV-1 Tat, this complex with inactive pTEFb further supports HIV-1 latency by preventing elongation of RNA polymerase II for active transcription [90]. Nevertheless,

459 it remains unknown if these mechanisms also apply to HIV-infected primary microglial
460 cells as transformed cells often behave quite differently.

461 In a previous study [37], we demonstrated that autocrine inflammatory cytokines
462 such as TNF-α were major drivers for spontaneous HIV reactivation in microglial cells,
463 and activation of GR with its specific ligands such as dexamethasone antagonized the
464 effects of cytokines on HIV reactivation [45]. However, we observed that the reactivated
465 HIV was subsequently silenced in microglial cells in the absence of dexamethasone,
466 suggesting the existence of additional HIV silencing mechanisms.

467 **Silencing of HIV by Nurr1 and CoREST**

468 In the present study, we identified the nuclear receptor Nurr1 as a key HIV silencing
469 factor. Overexpression of Nurr1 had little effect on preventing reactivation of latent HIV
470 but strongly enhanced silencing of active HIV after TNF-α stimulation and subsequent
471 withdrawal. Inversely, KD of endogenous Nurr1 in HC69 cells inhibited silencing of active
472 HIV after TNF-α withdrawal. Thus, results from both overexpression and KD experiments
473 unequivocally demonstrated a pivotal role of Nurr1 in silencing active HIV.
474 Mechanistically, we demonstrated that Nurr1 interacted with the
475 CoREST/HDAC1/G9a/EZH2 repressor complex as reported previously for cellular early
476 response genes [50]. Nurr1 promoted the recruitment of CoREST complexes to the HIV
477 promoter following TNF-α stimulation and subsequent withdrawal.

478 These epigenetic silencers likely silence active HIV by promoting histone de-
479 acetylation and repressive di- or tri-methylations. Consistent with this hypothesis,
480 functional inhibition with specific inhibitors or expressional KD or KO of each component
481 of the repressor complex including CoREST, G9a, and EZH2 strongly inhibited HIV

482 silencing. Data from RNA-Seq analysis indicated that Nurr1 might also utilize this "post-
483 TNF-α stimulation" epigenetic silencing mechanism to repress many host genes.

484 **Regulation of HIV latency in microglial cells by nuclear receptors**

485 Nuclear receptors are special transcription factors that turn on or turn off
486 expression of target genes upon specific ligand binding [91]. Accumulating evidence
487 suggest that nuclear receptors play an important role in regulating HIV expression. For
488 example, estrogen receptor (ER) and GR have been found to promote HIV latency in T
489 cells and microglial cells respectively [45, 63]. In this study, by using both immortalized
490 and iPSC-derived human microglial cells, we provided comprehensive data to
491 demonstrate that Nurr1 promoted HIV latency by silencing active HIV. In contrast, we did
492 not see significant effects of Nur77 and Nor1 overexpression on HIV when HC69 cells
493 were stimulated with TNF-α. However, we have not examined possible effects of these
494 nuclear receptors on HIV when microglial cells are activated through other signaling
495 pathways such as the "Toll-like" receptor signaling pathway [38]. In addition, it is well
496 known that the different Nerve Growth Factor IB-like nuclear receptors interact with each
497 other or with other nuclear receptors such as GR and the retinoid X receptors (RXR) [92,
498 93]. Therefore, in future experiments, we plan to investigate how Nur77, Nurr1, and Nor1
499 impact HIV expression in microglial cells in response to different stimuli and whether they
500 exert any synergistic effect on HIV expression between themselves or with other
501 interacting nuclear receptors.

502 **Role of Nurr1 in maintaining brain homeostasis**

503 The roles of Nerve Growth Factor IB-like nuclear receptors in brain development
504 and homeostasis are well established. Both Nor1 and Nurr1 are essential for

505 differentiation and survival of dopaminergic neurons [46-49]. Nurr1 deficiency in
506 embryonic ventral midbrain cells results in their failure to migrate and innervation of their
507 striatal target areas [94, 95]. Nurr1 deficiency or reduced expression due to mutations in
508 adults is a major contributing factor in the pathogenesis of Parkinson's disease [96]. Nurr1
509 is also expressed in non-neuronal cells including monocytes, macrophages, microglia,
510 and astrocytes. Its expression is reduced in the peripheral blood lymphocytes (PBL) of
511 patients with Parkinson's disease compared with healthy controls [97]. Lower levels of
512 Nurr1 in the brain and blood represents increased risks of Parkinson's disease and other
513 neurodegenerative diseases in adults [97].

514 Nurr1 protects dopaminergic neurons from inflammation-induced neurotoxicity
515 through the inhibition of pro-inflammatory mediator expression in microglia and astrocytes
516 by recruiting CoREST corepressor complexes to NF-κB target genes [50, 98]. A reduction
517 of Nurr1 expression in neurons does not affect their death but enhances expression of
518 inflammatory mediators, and the survival rate of neurons decreases in response to
519 inflammatory stimuli in the Nurr1 deficiency condition [50]. Multiple studies reported that
520 activation of Nurr1 reduces inflammation, protects neurons, and decreases Parkinson's
521 disease related symptoms [53, 65, 67, 99].

522 Although the pathogenesis of Parkinson's disease and other types of
523 neurodegeneration remains obscure, increasing evidence suggests that inflammatory
524 responses are responsible for the progression of most neurodegenerative diseases [100].
525 These responses include accumulation of inflammatory mediators, such as inflammatory
526 cytokines and proteases in the substantia nigra and the striatum, as well as activation of
527 the microglia [101], which are also common features of HAND [4, 102].

528 **Anti-inflammatory role for Nurr1 in HIV-infected microglial cells**

529 Little is known on how HIV infection impacts expression or functionality of Nurr1
530 and other nuclear receptors in the brain. Microglial activation is triggered by a series of
531 neurochemical mediators such as IFN-γ, inducible nitric oxide synthase (iNOS), IL-1β,
532 and TNF-α [103-106]. HIV infection of the brain likely further increases the levels of these
533 mediators. Interestingly, data from our RNA-Seq experiments reveal that Nurr1
534 overexpression pushed the activated microglial cells towards homeostasis following TNF-
535 α stimulation and subsequent withdrawal by repressing NF-κB signaling pathway and
536 genes involved in cellular activity and IFN-α and INF-γ responses. Thus, in addition to
537 silencing HIV, Nurr1 apparently plays a crucial role in suppression of microglia activation.
538 This finding is consistent with a recent report that glycolysis downregulation is a hallmark
539 of HIV-1 latency in microglial cells [107].

540 Further studies are warranted to determine the expression levels of these nuclear
541 receptors in HIV patients and investigate whether their deficiency or malfunction
542 contributes to development of HAND. Interestingly, multiple Nurr1 agonists exhibit strong
543 therapeutic effects and potentials for Parkinson's disease in pre-clinical animal study and
544 human trials [108]. In this study, we tested the Nurr1 agonists 6-MP and AQ. Both agents
545 strongly inhibited expression of HIV and the neurotoxin MMP2 in HC69 cells and iMGs.
546 In future studies, it would be of great interest to test additional agonists, particularly those
547 new generations of Nurr1 agonists currently on pre-clinical and human trials, for their anti-
548 HIV activity and eventual application in the clinic for treatment of HAND.

549

MATERIALS & METHODS

Chemicals and reagents

TNF-α (Invitrogen, Cat. #PHC3015) was used to induce HIV-1 reactivation in microglial cells. Nor1 and Nurr1 agonists 6-mercaptopurine (6-MP) (Millipore-Sigma, Cat#38171) and amodiaquine (AQ) (Millipore-Sigma, Cat#SMB00947) were used to activate the Nerve Growth Factor IB-like nuclear receptors. GSK343 (Sigma Aldrich, Cat# SML0766), UNC0638 (Sigma Aldrich, Cat#U4885), and suberoylanilide hydroxamic acid (SAHA, Millipore-Sigma, Cat#SML0061) were used to examine the effects of EZH2, H9a, and HDAC1/2 on HIV silencing respectively.

Numerous antibodies were used for Western blot analysis, co-immunoprecipitation (Co-IP), and chromatin immunoprecipitation (ChIP) assays, including a mouse monoclonal anti-FLAG M2 antibody (Sigma, Cat# F1804), a rabbit polyclonal anti-Nurr1 antibody (Sata Cruz Biotechnology, Cat# sc-991), a mouse monoclonal anti-Nurr1 antibody (Santa Cruz Biotechnology, Cat# sc-81345), a mouse monoclonal anti-Nor1 antibody (Perseus Proteomics, Cat# PP-H7833-00), a rabbit polyclonal anti-Nur77 antibody (Cell Signaling, Cat# 3960S), a rabbit monoclonal anti-MMP2 antibody (Cell Signaling, Cat#40994), a rabbit polyclonal anti-CoREST antibody (EMD Millipore, Cat# 07-579), a rabbit polyclonal anti-HDAC1 antibody (Santa Cruz Biotechnology, Cat# sc-7872), a rabbit polyclonal anti-G9a antibody (Cell Signaling, cat#3306S), a rabbit polyclonal anti-EZH2 antibody (Cell Signaling, Cat#5246S), a rabbit polyclonal anti-acetylated histone 3 (Ac-H3) antibody (Cell Signaling, Cat#9677S), a rabbit polyclonal anti-H3K27me3 antibody (EDM Millipore, Cat#07-449), a rabbit monoclonal anti-H3K27me2 antibody (Cell Signaling, Cat#9728S), a mouse monoclonal anti-HIV Nef

antibody (Abcam, Cat#ab42355), and a mouse monoclonal anti-RNA polymerase II antibody (Abcam, Cat#ab817).

Cells and flow cytometry analysis of HIV/GFP expression

HIV-1 infected immortalized human microglial (hμglia) HC69 cells were cultured and maintained as described as previously [37]. Induced pluripotent stem cells (iPSC)-derived human microglial cells (iMG) (Tempo Bioscience, Cat#SKU 1001.1) were plated, allowed to differentiate and maintained in culture on plates pre-coated with Matrigel matrix (Corning, Cat#356254) according to the manufacturer's instructions. The iMG were infected with EFGP HIV-1 reporter virus at 1 to 1 (cell-to-virus moiety), which was produced, purified, and titrated as described previously [37]. Two days after infection, the iMG were treated with and without the Nurr1 agonists 6-MP and AQ for four days. Infected with the same EGFP-reporter HIV-1 virus (**Fig 1 A**), HIV expression in hμglia and iMG cells was measured and quantified with percentage (%) of GFP+ cells by flow cytometry as described previously [45].

Lenti-viral construction and production, and generation of stable cell lines

Three lentiviral constructs, pLV[Bxp]-Bsd-CMV>3xFLAG-Nur77, pLV[Bxp]-Bsd-CMV>3xFLAG-Nurr1, and pLV[Bxp]-Bsd-CMV>3xFLAG-Nor1 were generated by inserting the full-length open reading frame (ORF) of human NR4A1 (Nur77), NR4A2 (Nurr1), and NR4A3 (Nor1) cDNA fragment into the empty vector pLV[Bxp]-Bsd-CMV>3xFLA immediately downstream of the Kozak sequence (VectorBuilder, vector ID: VB180227-1135bmn, VB180227-1134jht, and VB180227-1136rwc). The inserted cDNA was also "in frame" fused with the coding sequence of the N-terminal 3X-FLAG peptide tag, allowing to generate N-terminal 3xFLAG-tagged proteins. Two lentiviral constructs

596 expressing human Nurr1-specific shRNA (5'GGTTCGCACAGACAGTTTAAA3' and
597 5'ATACGTGTGTTTAGCAAATAA3'), one lentiviral construct expressing human
598 CoREST-specific shRNA (5'CCCAATAATGGCCAGAATAAA3'), and two lentiviral
599 constructs expressing control shRNAs (5'CCTAAGGTTAAGTCGCCCTCG3' and 5'
600 CAACAAGATGAAGAGCACCA3') were purchased from VectorBuilder. All lentiviral
601 constructs carried an ampicillin resistance gene for selection in bacteria (*E. coli*) and a
602 blasticidin resistance gene for selection of stable expression in mammalian cells.
603 Infectious viral particles with each of these lentiviral constructs were produced by co-
604 transfecting 293T cells with packaging plasmid psPAX2 (Addgene, Cat#12260) and Env
605 Vector pCMV-VSVg (Addgene, Cat#138479). HC69 cells stably expressing 3X-FLAG-
606 Nur77, 3X-FLAG-Nurr1, 3X-FLAG-Nor1, empty vector, gene-specific shRNA and control
607 shRNA were generated by infection of the cells with purified lentiviral particles for two
608 days, followed by culturing the cells in the presence of blasticidin at 10 μg/ml.

609 To investigate the effects of G9a and EZH2 on HIV silencing, we conducted
610 CRISPR/Cas9 mediated "knocking out" (KO) of these genes in HC69 cells, using a dual
611 CRISPR/Cas9 gRNA lentiviral vector. Two different guide RNAs targeting EZH2
612 (TGAGCTCATTGCGCGGGACT and GATCTGGAGGATCACCGAGA) or G9a
613 (TTCCCCATGCCCTCGCATCC and GTGGCAGCCCCACGGCTGAA) were cloned into
614 lentiCRISPR v2-Blast plasmid following the protocol described previously [109].
615 LentiCRISPR v2-Blast was a gift from Mohan Babu (Addgene plasmid # 83480). VSV-G
616 pseudotyped viruses expressing CRISPR/Cas9 gRNAs were produced in HEK 293T cells
617 by transfection of lentiCRISPR v2 plasmids together with psPAX2 and pCMV-VSV-G.
618 HC69 cells infected with the EZH2 or G9a KO lentiviruses were cultured in the presence

of blasticidin (10 μg/ml). Successful KO of these genes in HC69 cells were verified by Western blot analysis of EZH2 and G9a proteins in the resulting cell lines.

Reverse transcription and quantitative polymerase chain reaction (RT-qPCR)

Total RNAs from HC69 or HIV-infected IMG cells with different treatments were isolated by using the RNeasy Plus Mini kit from Qiagen (Cat#74134). The purified total RNAs were converted to first-strand cDNAs by using a reverse transcription kit (Bio-Rad, Cat#1708891). The relative levels of HIV-1 un-spliced transcript and human MMP-2 mRNA were measured by qRT-PCR using the primers 5'AGGGACCTGAAAGCGAAAG3' (HIV-1 un-spliced-forward) and 5'AATGATACGGCGACGACCNNNNNNNNNN3' (HIV-1 un-spliced-reverse), and 5'ATAACCTGGATGCCGTCGT-3′ (MMP2 forward) and AGGCACCCTTGAAGAAGTAGC-3′ (MMP2 reverse), respectively. The mRNA level of the housekeeping gene β-actin in each sample was used as reference for normalization, which was measured by qRT-PCR using the primers 5'-TCCTCTCCCAAGTCCACACAGG-3′ (forward) and 5'-GGGCACGAAGGCTCATCATTC-3′ (reverse). Each qRT-PCR was conducted in triplicates.

ChIP and ChIP-seq analyses

Standard procedures were followed for all ChIP assays. Briefly, cells were fixed with 1% Formaldehyde for 10 minutes (min) at room temperature, followed by incubation in PBS containing 125 mM glysine for 10 min at room temperature. After two washes with ice-cold PBS, cells were re-suspended and allowed to swell in CE buffer [10 mM Hepes, pH7.9, 60 mM KCl, 1 mM EDTA, 0.5% NP-40, 1 mM DTT] on ice for 10 min. After centrifugation at 2,000 g for 10 min at 4°C, nuclei were re-suspended in SDS lysis buffer [50 mM Tris-HCl, 1 mM EDTA, 0.5% SDS] and incubated on ice for 10 min. Sheared

chromatins were prepared by sonicating the nuclei lysate to generate DNA fragments in the range of 250 to 500 bps. ChIP assays with specific antibodies were carried out in ChIP dilution buffer [16.7 mM Tris-HCl, pH 8.1, 167 mM NaCl, 1.2 mM EDTA, 1.1% Triton X-100, and 0.01% SDS] containing 5 μg antibody and 50 ul protein-A/protein-G magnetic beads per reaction at 4°C for overnight with rotation, followed by consecutive washes with low salt wash buffer [20mM Tris-HCl, pH8.1, 150 mM NaCl, 1 mM EDTA, 1% Triton X-100, 0.1% SDS], high salt wash buffer [20mM Tris-HCl, pH8.1, 500 mM NaCl, 1 mM EDTA, 1% Triton X-100, 0.1% SDS], and RIPA buffer [20 mM Tris-HCl, pH7.5, 150 mM NaCl, 5 mM EDTA, 0.5% Triton X-100, 0.5% sodium deoxycholate, and 0.1% SDS]. The washed beads were then re-suspended in elution buffer [50 mM Tris-HCl, pH 6.5, 20 mM NaCl, 100 mM NaHCO3, 1 mM EDTA, 1% SDS, 100 μg/ml proteinase K] and incubated at 50°C for 2h. Supernatants from the beads were collected and used for ChIP DNA purification using Qiagen's PCR purification kit (Cat#28104). Quantification of input and ChIP DNA corresponding to HIV-1 promoter region was conducted by qPCR using specific primers as reported previously [110].

For ChIP-seq analyses, the DNA products from each ChIP assay were first end repaired with end repair enzyme mix (New England Biolabs, Inc., Cat#M6630), then ligated to NEBNext adaptor included in the NEBNext® Ultra™ II DNA Library Prep Kit for Illumina® (Cat#E7645L) according to the manufacturer's instruction, followed by PCR amplification with a specific pair of bar-coded primers. Next, to enrich HIV-1 specific sequences in the library, DNA samples from all ChIP assays were pooled, denatured at 98°C for 10 min, and then subjected to hybridization with 50 times excessive amount of biotin-labelled and pre-denatured HIV-1 genomic DNA in hybridization buffer containing

5XSSC and salmon sperm DNA (100 μg/ml) at 65°C for 1 h. Fragments hybridizing to biotin-labelled HIV-1 DNA were pulled down by incubating the hybridization reaction with streptavidin-conjugated magnetic beads (ThermoFisher Scientific, Cat#88816) at room temperature for 30 min, followed by three times washes with ion wash buffer and elution in water. The enriched ChIP library DNA was PCR amplified with Ion A and Ion P1 primers, and PCR fragments in the range from 300 to 500 bps were purified from agarose gel after electrophoresis and loaded for Ion Torrent sequencing.

We aligned the sequence reads to NL4.3-Cd8a-EGFP-Nef+ HIV-1 genome. Raw fastq sequencing data were imported to *the public server at usegalaxy.org for analysis* [111]. We used FASTX-Toolkit for deconvolution of reads. Read mapping was performed by Bowtie2 tool with default settings using the NL4.3-Cd8a-EGFP-Nef+ HIV-1 as a reference genome [112, 113]. DeepTool2 was used to make graphs for distribution of mapped reads along HIV-1 genome [114].

RNA-Seq and data analysis

Approximately 2 million GFP-negative cells from each of the cell lines HC69-3X-FLAG-vector, HC69-3X-FLAG-Nor1, HC69-3X-FLAG-Nurr1, HC69-control shRNA, and HC69-Nurr1 shRNA were collected from sorting. The isolated cells were expanded in DMEM culture media with low glucose (1g/L) and 1% FBS for 48 hr in the presence of dexamethasone (1μg/ml) to maintain HIV latency as reported previously [45]. The cells were next cultured in fresh medium without dexamethasone, un-treated, or treated with low dose (20 pg/ml) and high dose (400 pg/ml) TNF-α for 24 h. One portion of the cells treated with high dose TNF-α were washed twice with PBS, followed by culturing in fresh medium in the absence of TNF-α and dexamethasone for 48 h. Total RNAs from each

cell line with different treatments were isolated by using the RNeasy Plus Mini kit from Qiagen (Cat#74134). The isolated RNAs were treated with RNase-free DNAse I at 37 °C for 30 min to remove genomic DNA, followed by a second-round purification using the same RNA purification kit. For reproducibility concerns, the RNA-Seq analysis consisted of RNA samples from two independent experiments performed several months apart.

Total cellular RNA was subjected to 150 base long, paired end RNA-Seq on an NovaSeq 6000 instrument. RNA-Seq reads were quality controlled using Fastqc and trimmed for any leftover adaptor-derived sequences, and sequences with Phred score less than 30 with Trim Galore, which is a wrapper based on Cutadapt and FastQC. Any reads shorter than 40 nucleotides after the trimming was not used in alignment. The pre-processed reads were aligned to the human genome (hg38/GRCh38) with the Gencode release 28 as the reference annotations using STAR version 2.7.2b [115], followed by gene-level quantitation using htseq-count [116]. In parallel, the pre-processed reads were pseudoaligned using Kallisto version 0.43.1 [117], with 100 rounds of bootstrapping to the Gencode release 28 of the human transcriptome to which the sequence of the transfected HIV genome and the deduced HIV spliced transcripts were added. The resulting quantitations were normalized using Sleuth. The two pipelines yielded concordant results. Pairwise differential expression tests were performed using generalized linear models as implemented in edgeR (QL) [118], and false discovery rate (FDR) values were calculated for each differential expression value.

Protein-coding genes that were expressed at a minimum abundance of 5 transcripts per million (TPM) were used for pathway analysis with fold change values as the ranking parameter while controlling false discovery rate at 0.05. Gene Set Enrichment

Analysis (GSEA) package was used to identify the enriched pathway and promoter elements using mSigDB and KEGG databases. Pathways that showed an FDR q-value <= 0.25 were considered significantly enriched, per the GSEA package guidelines. The number of genes contributing to the enrichment score was calculated using the leading edge output of GSEA (tag multiplied by size).

Identification of marker genes for each study group

After filtration of the raw reads to remove low quality reads and mapping the clean reads to the human reference genome using STAR software, differential analysis was performed by edgeR package. For RNA-Seq data analysis, the bulk RNA-Seq data in a form of digital gene expression (DGE) matrix was analyzed using the Seurat package for R, v. 3.1.5 [119]. Variable genes were identified using the *FindVariableFeatures* function. Top fifteen markers for each cluster were identified using a Wilcoxon Rank Sum test, and a heat map was generated using the *DoHeatmap* function.

SUPPORTING INFORMATION

S1 Fig. Nurr1 overexpression (OE) or knock-down (KD) substantially alters host transcriptome. **A**, heatmaps representing top 15 gene markers for each treatment group. Statistically-significant ($p < 0.001$) differentially expressed genes were determined using the Wilcoxon rank-sum test reflecting the impacts of Nurr1 OE by comparing the control cells HC69-3X-FLAG-vector (VT) with Nurr1 overexpressing cells HC69-3X-FLAG-Nurr1 (Nurr1 OE), as well as the impacts of KD by comparing the HC69-control shRNA1 and control shRNA2 (Ctl shRNA1/2) cells with HC69-Nurr1 shRNA1 and shRNA2 (Nurr1 shRNA1/2) cells, respectively. Various cell lines were cultured in the absence (untreated) or presence of high dose (400 pg/ml) TNF-α for 24 hr. In addition, cells were given 48 hr chase after stimulation with high dose (400 pg/ml) TNF-α for 24 hr and subsequent withdrawal. **B**, heatmaps showing top 15 gene transcript markers in samples from panel **A** rearranged according to their status of treatment with TNF-α.. The most enriched gene transcripts as the result of Nurr1 overexpression or KD are listed in columns to the left. The color-coded expression pattern of each gene transcript is shown in a heatmap to the right.

S2 Fig. **Nurr1 overexpression mainly impacts the recovery step following TNF-α stimulation.** Trajectories of genes after stimulation with low dose (20 pg/ml) and high dose (400 pg/ml) TNF-α for 24 hr and following a 48 hr recovery (chase) after high dose TNF-α stimulation for 24 hr and subsequent withdrawal in the Nurr1 overexpression cell line HC69-3X-FLAG-Nurr1 (Nurr1 OE) were shown. Trajectories of the same genes in the control cell line HC69-3X-FLAG-vector (Ctl VT) were also shown, with a semi-transparent line connecting identical genes between the control and Nurr1-overexpressing sides of

each graph. Each line represented a gene, and the Y axis values indicated the log2 expression levels. The number of genes showing each trajectory in Nurr1-overexpressing cells was shown on top. Genes that showed no change, were up regulated, and down regulated in statistically significant manner (FDR<0.05, fold change>2) were indicated with the letters n, u, and d respectively. Grouping of the different trajectories was based on gene responses during stimulation with low dose (Step 1) and high dose (Step 2) TNF-α and the recovery time after TNF-α stimulation and subsequent withdrawal (Step 3). For instance, the group of genes marked “ndu” represented genes that were not significantly changed in response to stimulation with low dose TNF-α but were down regulated with high dose TNF-α stimulation and then up regulated during the recovery (chase) period.

S3 Fig. **HC69-3X-FLAG-Nurr1 and HC69-3X-FLAG-vector cells strongly differ in the recovery step following TNF-α stimulation**. Genes that showed a different trajectory after TNF-α stimulation for 24 hr and following a 48 hr recovery period between HC69-3X-FLAG-vector (control) and HC69-3X-FLAG-Nurr1 cells were identified and groups containing over 100 genes were graphed. Each line represented a gene and a semi-transparent line connected identical genes between control and Nurr1-overexpressing sides of each graph. The Y axis indicated the expression level of each gene throughout the trajectory. Grouping of genes with no statistically significant changes in expression (n), up regulated (d), or down regulated (d) in the three segments was as described in **S2 Fig**.

S4 Fig. Nurr1 overexpression (OE) substantially alters host transcriptome. Genes involved in top differentially negatively enriched pathways in **Fig 6A** are shown in heatmaps. The values shown in the heatmap correspond to the level of differential

771 expression between Nurr1 overexpressing cells (marked as “Nurr1”) versus vector-
772 infected control cells (marked as “Vector”) during the chase step. The identities of the
773 plotted pathways and genes involved in the pathways are shown on the top and to the
774 right, respectively.

775 **S5 Fig. Nurr1-specific gene expression during the chase step leads to strong**
776 **downregulated of genes involved in cell cycle.** Genes that exclusively change in
777 expression during the chase step only in Nurr1 cells (see **S3 Fig**) were superimposed on
778 the KEGG cell cycle graph. The color bar on the top right indicates the level of differential
779 expression for each gene in Nurr1 cells during the chase step.

780 **S6 Fig. TNF-α stimulation leads to strong induction of NF-κB-responsive genes**
781 **along with targets of multiple inflammatory cytokines.** The most enriched
782 transcription factor binding motifs in proximity of the promoters of differentially expressed
783 genes are shown. The size of the circles indicates the level of enrichment, while the color
784 intensity reflects the statistical significance as shown by FDR. Positively- and negatively-
785 enriched motifs are shown after each treatment (shown at the bottom) in the left and right
786 panel, respectively. The identity of each motif, as annotated in the C3 lists of the MSIGDB
787 database, is shown to the left.

788 **S7 Fig. Nurr1 associates with CoREST, HDAC1, G91, and EZH2 to form a**
789 **transcription repression complex in microglial cells (HC69).** HC69-3X-FLAG-vector
790 and HC69-3X-FLAG-Nurr1 cells were cultured in the absence (untreated) or presence of
791 high dose (400 pg/ml) TNF-α for 4 hr and 24 hr respectively. A portion of these cells were
792 also used in a chase experiment by culturing the cells for an additional 24 hr (chase) after
793 stimulation with high dose TNF-α for 24 hr and subsequent washing with PBS (TNF-α

794 24h+24h). Total protein lysates from the differently treated cells were isolated and used
795 for co-immunoprecipitation (Co-IP) with a mouse anti-FLAG monoclonal antibody. The
796 original protein lysates (Input) and the Co-IP products were analyzed by Western blot
797 analysis with antibodies to FLAG, CoREST, HDAC1, G9a, EZH2, and β-tubulin
798 respectively.
799

ACKNOWLEDGEMENT

This study was supported by NIH grants R01 DA043159 and R01 DA049481 to J.K. and R21-AI127252 and two Development Awards from CFAR P30-AI36219 to S.V. We thank Meenakhi Shukla for technical assistance for production of HIV-1 reporter virus. This work made use of the High Performance Computing Resource for Advanced Research Computing and flow cytometry and virology cores of the Center for AIDS Research (CFAR) at Case Western Reserve University.

AUTHOR CONTRIBUTIONS

J.K., F.Y. and D.A. conceived of and oversaw the study. F.Y. performed all the wet bench experiments in the manuscript except as noted and along with J.K., wrote the manuscript. D.A. performed the culture of iPSC derived microglial cells and participated in data analysis and manuscript preparation. K.N. constructed the gene knock out lentiviruses and performed the ChIP-seq data analysis. S.V. processed and analyzed the RNA-Seq dataset and performed the trajectory studies and pathway analysis, participated in manuscript preparation and submitted the RNA-Seq studies performed in this project to SRA (accession number to be provided). K.L. performed the marker gene discovery for the RNA-Seq data. Y.G. performed microglial cell culture and participated in data analysis. S.S. performed the culture of iPSC derived microglial cell and participated in data analysis. All authors read the final manuscript and commented on it.

FIGURE LEGENDS

Figure 1. Spontaneous silencing of active HIV in microglial cells. A, genome organization of a d2EGFP reporter HIV-1 that was cloned in the lentiviral vector pHR'. A fragment of HIV-1_{pNL4-3}, containing *Tat*, *Rev*, *Env*, *Vpu* and *Nef* with the green fluorescence reporter gene d2EGFP, was cloned into the lentiviral vector pHR'. The resulted plasmid was used to produce the VSV-G HIV particles as described previously [120]. Immortalized human microglial cells (hμglia) were infected with the lenti-HIV viral particles, generating multiple clones with an integrated pro-virus genome. HC69 was a representative of these clones. **B,** Schematic diagram of experimental scheme to study the role of nuclear receptors in microglial reactivation and reversion to latency. **C,** Representative phase contrast, GFP, and overlapped images of HC69 cells that were cultured in the absence (untreated, left panel) and in the presence of TNF-α (400 pg/ml) for 24 hr (TNF-α 24 h, middle panel) respectively, or used in a chase experiment by continuously culturing HC69 cells in the absence of TNF-α for 96 hr after stimulating the cells with TNF-α (400 pg/ml) for 24 hr and washing with PBS (TNF-α 24 h+96 h, right panel). The average percentages of GFP+ cells indicated for each panel were measured by flow cytometry from triplicate wells.

Figure 2. Activation of Nurr1 enhances HIV silencing in immortalized human microglial cells (hμglia). A, Impact of Nurr1 agonist 6-MP on HIV expression. Left: Representative flow cytometry histograms. Right: Quantitative results from three independent experiments. For this experiment, we used a batch of HC69 cells with high numbers of GFP^+ cells resulting from spontaneous HIV reactivation following multiple passages of culture in the absence of dexamethasone. These cells were cultured in the

844 presence of different doses of 6-MP for three days. The percentages of GFP^+ cells from
845 the differently treated cells were measured by flow cytometry. The *p*-values of pair-
846 sample, Student's *t*-tests comparing un-treated cells and cells treated with different
847 doses of 6-MP were calculated from three independent experiments. **B**, Western blot
848 detection of Nurr1, Nor1, HIV-1 Nef protein, and Nurr1 target gene MMP2 in HC69 cells
849 described in A. The level of β-tubulin was used as a loading control. **C**, the nuclear
850 receptor agonists dexamethasone (DEXA, 1 μM), Bexarotene (BEX, 1 μM) and 6-MP (1
851 μM) have additive effects on HIV silencing in HC69 cells. HC69 cells were first treated
852 with high dose (400 pg/ml) TNF-α for 24 hr, followed by a 72 hr chase experiment during
853 which the cells were washed with PBS and cultured in fresh media in the presence of
854 placebo (DMSO) or the various NR agonists, alone or in combination. Expression of Nef
855 and β-tubulin in the differently treated cells was analyzed by Western blot analysis as
856 described in C.

857 **Figure 3. Overexpression of Nurr1 in HC69 cells enhances HIV silencing. A,**
858 RNA-Seq confirmation of overexpression (OE) of Nurr1 in HC69 cells. Sequence read
859 histograms for the Nurr1 locus is shown for control (vector) and Nurr1 overexpression.
860 Annotated genes for the shown locus are indicated on the top, and the position of the
861 locus on chromosome 2 is shown both at the top and the bottom. A read scale for each
862 row is shown on the right, with the values for the overexpression studies drawn on a log2
863 scale. **B,** Verification of Nur77, Nurr1, and Nor1 overexpression by Western blot analysis
864 in HC69 cell lines stably expressing 3X-FLAG-tagged Nur77, Nurr1, and Nor1
865 respectively. HC69 cells stably carrying the 3X-FLAG-empty vector were used as a
866 reference for comparison. The level of β-tubulin was used as a loading control. Notably,

867 the levels of endogenous Nur77 and Nor1 in HC69 cells were very limited. In contrast,
868 Nurr1 was constitutively expressed in HC69 cells. **C,** Schematic depicting the TNF-α
869 stimulation and chase studies. The four cell lines described in B were either untreated or
870 treated with high dose (400 pg/ml) TNF-α for 24 h. To examine HIV silencing, one set of
871 TNF-α induced cells were used in a chase experiment by continuous culture of the cells
872 in the absence of TNF-α for an additional 48 h. The time points at which TNF-α is added
873 or removed are shown by arrows on the top. **D,** Expression of HIV Nef protein in the
874 different cell lines before and after TNF-α stimulation and at the end of the chase
875 experiment was measured by Western blot analysis. The level of β-tubulin was used as
876 a loading control. **E,** Expression level of HIV mRNA (black bar graph) and Nurr1 (red
877 rectangles and lines) in transcripts per million cellular transcripts are shown for each of
878 the treatment steps shown in panel C in both vector-infected cells (on the left) and Nurr1
879 overexpressing cells (on the right half of the graph). For the 24 hr TNF-α stimulation step,
880 both a low dose (20 pg/ml) and a high dose (400 pg/ml) are used. The values shown are
881 the average of three replicate RNA-Seq samples with two standard deviations as error
882 bars. The expression values for HIV and Nurr1 are shown on Y axes to the left and right,
883 respectively.

884 **Figure 4. Nurr1 knock down (KD) in HC69 cells enhances HIV expression and**
885 **block proviral silencing during the chase step. A,** RNA-Seq confirmation of Nurr1 KD
886 in HC69 cells. Read histograms for the Nurr1 locus is shown for non-targeting shRNA-
887 infected cells, and cells infected with Nurr1 specific shRNA lentiviral constructs.
888 Annotated genes for the shown locus are indicated on the top, and the position of the
889 locus on chromosome 2 is shown both at the top and the bottom. A read scale for each

row is shown on the right, with the values for the knock down studies drawn on a linear scale. **B,** Schematic depicting the TNF-α stimulation and chase studies. The two shRNA lentiviral transduced cell lines described in A were either untreated or treated with high dose (400 pg/ml) TNF-α for 24 hr. One set of TNF-α induced cells were used in a chase experiment in the absence of TNF-α for an additional 48 hr. The time points at which TNF-α is added or removed are shown by arrows on the top. **C,** Western blot studies measuring the expression of endogenous Nurr1, Nef, and β-tubulin in cells infected with either a non-targeting control shRNA or Nurr1-specific shRNA lentiviral vectors. The expression patterns from the TNF-α (400 pg/ml) stimulation and the chase step are shown. **D,** KD of endogenous Nurr1 strongly inhibits HIV silencing. The percentages of GFP^+ cells in the two cell lines, before treatment, at 24 hr post-TNF-α (400 pg/ml) stimulation, and at 72 hr after TNF-α withdrawal (chase) were analyzed by flow cytometry and calculated from three independent experiments. The difference in GFP expression between the two cell lines at 72 hr chase was statistically significant, with a $p = 0.0078$. **E,** Expression level of Nurr1 (red rectangles and lines) and the HIV provirus (black bar graph) in transcripts per million cellular transcripts are shown for each of the treatment steps in both non-targeting shRNA infected cells (on the left) and Nurr1-specific shRNA-infected cells (on the right half of the graph). The values shown reflect the average of three replicate RNA-Seq samples from two distinct shRNA constructs per control and Nurr1 knock down groups, with two standard deviations as error bars. The expression values for HIV and Nurr1 are shown on Y axes to the left and right, respectively.

Figure 5. Nurr1 overexpression leads to the inhibition of critical cellular proliferation pathways. A, Patterns of differential gene expression during the chase step

913 in vector-infected (top) and Nurr1 overexpressing (Nurr1 OE) cells. Dotted lines indicate
914 the two-fold cut off level. **B,** Pathway analyses of Nurr1 overexpression at baseline, during
915 TNF-α stimulation, and following the recovery period after TNF-α stimulation. The
916 identities of specific highly enriched pathways are shown on the Y axis, and the
917 comparisons are shown at the bottom. The color and size of circles correspond to
918 statistical significance, as shown by FDR, and normalized enrichment values,
919 respectively. Positive and negatively enriched pathways are shown in the left and right
920 plot, respectively.

921 **Figure 6. Nurr1 overexpression accelerates homeostasis of activated**
922 **microglial cells by shutting down pathways involved in the maintenance of cellular**
923 **activation and inflammation. A,** Identification of genes selectively altered as a result of
924 Nurr1 overexpression (Nurr1 OE), compared to the control empty vector (Ctl VT) cells, by
925 trajectory analysis. Genes that are unaltered (n), downregulated (d) or upregulated (u)
926 were identified during the activation and the chase steps and were clustered into families
927 with similar profiles. The total number of genes in each category is indicated for both the
928 control and Nurr1-overexpressing cells. Note that the major differences in the gene
929 expression profiles are seen in genes that are either upregulated or downregulated during
930 the chase (highlighted by asterisks). To enable the visualization of the trajectories with
931 low, medium and high membership, the X axis for each group is shown separately. **B,**
932 Pathway analysis using the Hallmark gene lists of the MSigDB database was performed
933 on non-TNF-α-responsive genes that are exclusively altered in expression during the
934 chase step in Nurr1 overexpressing cells, corresponding to genes which follow nnu and
935 nnd trajectories in Nurr1 cells and an nnn trajectory in control cells (see **S3 Fig**). The

identity of each pathway is shown to the left, and the direction of enrichment (+ or -) is shown at the bottom. The color and size of circles corresponded to statistical significance, as shown by FDR, and normalized enrichment values, respectively.

Figure 7. Nurr1 promotes recruitment of the CoREST repressor complex to HIV promoter. A, Schematic illustration of Nurr1-mediated epigenetic silencing of active HIV in microglial cells by recruiting the CoREST/HDAC1/G9a/EZH2 repression complex to HIV promoter. **B,** ChIP-seq signals (numbers of sequence reads on Y axis) along the reporter HIV-1 pro-viral genome (Figure 1A) on the X axis, resulting from ChIP-seq analysis with antibodies to EZH2, G9a, HDAC1, CoREST, and control IgG, respectively, and sheared chromatins prepared from HC69 cells that were un-treated, induced with TNF-α (400 pg/ml) for 4 hr and 24 hr respectively, or used in a chase experiment by continuously culturing HC69 cells in the absence of TNF-α for 24 hr after stimulating the cells with TNF-α (400 pg/ml) for 24 hr and washing with PBS. Construction of ChIP-seq DNA libraries with the ChIP products, enrichment for HIV-1 specific sequences, and data analysis following Ion Torrent sequencing were described in Materials & Methods. Positions of ChIP sequence reads along the viral genome were marked. **C & D**, levels of CoREST (C) and G9a (D) in HIV 5'LTR (+30 to +134) in HC69-control shRNA (Control) and HC69-Nurr1 shRNA (Nurr1 KD) cell lines that were treated as described in B. The levels of CoREST and G9a in HIV 5'LTR were measured by qPCR and calculated as percentages of the amounts of ChIP products over input DNA from triplicate qPCR.

Figure 8. The CoREST repressor complex plays a pivotal role in silencing active HIV in microglial cells. A, Inhibition of HDAC1, G9a, and EZH2 blocked silencing of activated HIV in HC69 cells. HC69 cells were stimulated with high dose (400 pg/ml)

959 TNF-α for 24 hr. After washing with PBS, the cells were cultured in the presence of DMSO
960 (placebo, Control), HDAC inhibitor SAHA (2 μM), G9a inhibitor UNC0638 (2.5 μM), and
961 EZH2 inhibitor GSK343 (2.5 μM), respectively, for 48 hr. The levels of GFP expression
962 for each treatment were measured by flow cytometry and calculated from three
963 independent experiments, with *p* values between the control and treatment with each
964 inhibitor indicated. **B,** Verification of CoREST KD by Western blot detection of CoREST
965 protein expression in HC69 cell lines stably expressing control shRNA or CoREST-
966 specific shRNA. **C,** Verification of EZH2 and G9a KO by Western blot detection of G9a
967 and EZH2 protein expression in HC69 cells stably expressing CRISPR/Cas9 and G9a or
968 EZH2 specific gRNA, which were compared to the control HC69 cells stably expressing
969 CRISPR/Cas9 without gRNA. β-tubulin was used as a loading control for all Western blot
970 analysis. **D,** CoREST KD prevents HIV silencing. The HC69-control shRNA and HC69-
971 CoREST-shRNA cells were untreated, induced with high dose (400 pg/ml) TNF-α for 24
972 hr, or used in a chase experiment by continuous culturing the cells for 48 hr after TNF-α
973 stimulation for 24 hr and washes with PBS. GFP expression levels of all cells were
974 measured by flow cytometry and the mean values were calculated from three
975 independent experiments. Significant differences were observed between the HC69-
976 control shRNA and HC69-CoREST shRNA cell lines. **E,** G9a and EZH2 KO prevents HIV
977 silencing. Evaluation of the HC69 cell lines expressing G9a or EZH2 specific gRNA or
978 empty vector by flow cytometry following the same protocol as in panel D. There was a
979 significant difference between HC69-vector and HC69 EZH2 or G9a KO cell lines at 48
980 hr after TNF-α withdrawal, with $p < 0.01$.

Figure 9. Nurr1 Mediates HIV silencing in iPSC-derived microglial cells (iMG). **A,** Representative phase contrast, GFP, and overlapped images of iMG that were un-infected or infected with the reporter HIV-1 shown in Fig 1A, at 48 hr post-infection (hpi). HIV-infected iMG were treated with different doses of Nurr1 agonist 6-MP or AQ for four days, followed by flow cytometry analysis of GFP expression. **B,** The average levels of GFP expression in iMG treated with various doses of 6-MP. **C,** The average levels of GFP expression in iMG treated with various doses of AQ were calculated from three replicates. **D,** The levels of HIV RNA (un-spliced) in the cells described in panels A and B, were measured by RT-qPCR. **E,** The mRNA level of Nurr1 target gene MMP2 in the same cells was measured by qRT-PCR. The average levels of HIV transcript and MMP2 mRNA in each sample were calculated from triplicates of qRT-qPCR. Differences in HIV and MMP2 mRNA levels between un-treated cells and cells treated with different doses of 6-MP or AQ were statistically significant (** *p*-values <0.001). HIV transcripts were only detected in infected iMG cells (panel D). MMP2 mRNA was significantly elevated in HIV infected iMG (panel E).

997 **REFERENCES**

998 1. Resnick L, Berger JR, Shapshak P, Tourtellotte WW. Early penetration of the
999 blood-brain-barrier by HIV. Neurology. 1988;38(1):9-14. Epub 1988/01/01. doi:
1000 10.1212/wnl.38.1.9. PubMed PMID: 3422110.

1001 2. Achim CL, Schrier RD, Wiley CA. Immunopathogenesis of HIV encephalitis. Brain
1002 pathology (Zurich, Switzerland). 1991;1(3):177-84. Epub 1991/04/01. doi:
1003 10.1111/j.1750-3639.1991.tb00657.x. PubMed PMID: 1669706.

1004 3. Castellano P, Prevedel L, Eugenin EA. HIV-infected macrophages and microglia
1005 that survive acute infection become viral reservoirs by a mechanism involving Bim.
1006 Scientific reports. 2017;7(1):12866. Epub 2017/10/11. doi: 10.1038/s41598-017-12758-
1007 w. PubMed PMID: 28993666; PubMed Central PMCID: PMCPMC5634422.

1008 4. Wallet C, De Rovere M, Van Assche J, Daouad F, De Wit S, Gautier V, et al.
1009 Microglial Cells: The Main HIV-1 Reservoir in the Brain. Front Cell Infect Microbiol.
1010 2019;9:362. Epub 2019/11/12. doi: 10.3389/fcimb.2019.00362. PubMed PMID:
1011 31709195; PubMed Central PMCID: PMCPMC6821723.

1012 5. Dunfee R, Thomas ER, Gorry PR, Wang J, Ancuta P, Gabuzda D. Mechanisms of
1013 HIV-1 neurotropism. Current HIV research. 2006;4(3):267-78. Epub 2006/07/18. doi:
1014 10.2174/157016206777709500. PubMed PMID: 16842080.

1015 6. Eggers C, Arendt G, Hahn K, Husstedt IW, Maschke M, Neuen-Jacob E, et al. HIV-
1016 1-associated neurocognitive disorder: epidemiology, pathogenesis, diagnosis, and
1017 treatment. J Neurol. 2017;264(8):1715-27. Epub 2017/06/02. doi: 10.1007/s00415-017-
1018 8503-2. PubMed PMID: 28567537; PubMed Central PMCID: PMCPMC5533849.

1019 7. Clements JE, Gama L, Graham DR, Mankowski JL, Zink MC. A simian
1020 immunodeficiency virus macaque model of highly active antiretroviral treatment: viral
1021 latency in the periphery and the central nervous system. Curr Opin HIV AIDS.
1022 2011;6(1):37-42. Epub 2011/01/19. doi: 10.1097/COH.0b013e3283412413. PubMed
1023 PMID: 21242892; PubMed Central PMCID: PMCPMC3215305.

1024 8. Desplats P, Dumaop W, Smith D, Adame A, Everall I, Letendre S, et al. Molecular
1025 and pathologic insights from latent HIV-1 infection in the human brain. Neurology.
1026 2013;80(15):1415-23. Epub 2013/03/15. doi: 10.1212/WNL.0b013e31828c2e9e.
1027 PubMed PMID: 23486877; PubMed Central PMCID: PMC3662272.

1028 9. Brew BJ, Barnes SL. The impact of HIV central nervous system persistence on
1029 pathogenesis. AIDS (London, England). 2019;33 Suppl 2:S113-S21. Epub 2019/12/04.
1030 doi: 10.1097/QAD.0000000000002251. PubMed PMID: 31790377.

1031 10. Brew BJ, Chan P. Update on HIV dementia and HIV-associated neurocognitive
1032 disorders. Curr Neurol Neurosci Rep. 2014;14(8):468. Epub 2014/06/19. doi:
1033 10.1007/s11910-014-0468-2. PubMed PMID: 24938216.

1034 11. Glass JD, Fedor H, Wesselingh SL, McArthur JC. Immunocytochemical
1035 quantitation of human immunodeficiency virus in the brain: correlations with dementia.
1036 Annals of neurology. 1995;38(5):755-62. Epub 1995/11/01. doi: 10.1002/ana.410380510.
1037 PubMed PMID: 7486867.

1038 12. Masliah E, Heaton RK, Marcotte TD, Ellis RJ, Wiley CA, Mallory M, et al. Dendritic
1039 injury is a pathological substrate for human immunodeficiency virus-related cognitive
1040 disorders. HNRC Group. The HIV Neurobehavioral Research Center. Annals of
1041 neurology. 1997;42(6):963-72. Epub 1997/12/24. doi: 10.1002/ana.410420618. PubMed
1042 PMID: 9403489.

1043 13. Gannon P, Khan MZ, Kolson DL. Current understanding of HIV-associated
1044 neurocognitive disorders pathogenesis. Curr Opin Neurol. 2011;24(3):275-83. Epub
1045 2011/04/07. doi: 10.1097/WCO.0b013e32834695fb. PubMed PMID: 21467932; PubMed
1046 Central PMCID: PMCPMC3683661.

1047 14. Jurga AM, Paleczna M, Kuter KZ. Overview of General and Discriminating Markers
1048 of Differential Microglia Phenotypes. Frontiers in cellular neuroscience. 2020;14:198.
1049 Epub 2020/08/28. doi: 10.3389/fncel.2020.00198. PubMed PMID: 32848611; PubMed
1050 Central PMCID: PMCPMC7424058.

1051 15. Zhou T, Huang Z, Sun X, Zhu X, Zhou L, Li M, et al. Microglia Polarization with
1052 M1/M2 Phenotype Changes in rd1 Mouse Model of Retinal Degeneration. Front
1053 Neuroanat. 2017;11:77. Epub 2017/09/21. doi: 10.3389/fnana.2017.00077. PubMed
1054 PMID: 28928639; PubMed Central PMCID: PMCPMC5591873.

1055 16. Alsema AM, Jiang Q, Kracht L, Gerrits E, Dubbelaar ML, Miedema A, et al. Profiling
1056 Microglia From Alzheimer's Disease Donors and Non-demented Elderly in Acute Human
1057 Postmortem Cortical Tissue. Front Mol Neurosci. 2020;13:134. Epub 2020/11/17. doi:
1058 10.3389/fnmol.2020.00134. PubMed PMID: 33192286; PubMed Central PMCID:
1059 PMCPMC7655794.

1060 17. Mesquida-Veny F, Del Rio JA, Hervera A. Macrophagic and microglial complexity
1061 after neuronal injury. Progress in neurobiology. 2021;200:101970. Epub 2020/12/29. doi:
1062 10.1016/j.pneurobio.2020.101970. PubMed PMID: 33358752.

1063 18. Miedema A, Wijering MHC, Eggen BJL, Kooistra SM. High-Resolution
1064 Transcriptomic and Proteomic Profiling of Heterogeneity of Brain-Derived Microglia in
1065 Multiple Sclerosis. Front Mol Neurosci. 2020;13:583811. Epub 2020/11/17. doi:
1066 10.3389/fnmol.2020.583811. PubMed PMID: 33192299; PubMed Central PMCID:
1067 PMCPMC7654237.

1068 19. Sheeler C, Rosa JG, Ferro A, McAdams B, Borgenheimer E, Cvetanovic M. Glia
1069 in Neurodegeneration: The Housekeeper, the Defender and the Perpetrator. Int J Mol Sci.
1070 2020;21(23). Epub 2020/12/06. doi: 10.3390/ijms21239188. PubMed PMID: 33276471;
1071 PubMed Central PMCID: PMCPMC7730416.

1072 20. Avedissian SN, Dyavar SR, Fox HS, Fletcher CV. Pharmacologic approaches to
1073 HIV-associated neurocognitive disorders. Curr Opin Pharmacol. 2020;54:102-8. Epub
1074 2020/10/14. doi: 10.1016/j.coph.2020.09.003. PubMed PMID: 33049585; PubMed
1075 Central PMCID: PMCPMC7770011.

1076 21. Neumann H, Kotter MR, Franklin RJ. Debris clearance by microglia: an essential
1077 link between degeneration and regeneration. Brain : a journal of neurology. 2009;132(Pt
1078 2):288-95. Epub 2008/06/24. doi: 10.1093/brain/awn109. PubMed PMID: 18567623;
1079 PubMed Central PMCID: PMCPMC2640215.

1080 22. Nimmerjahn A, Kirchhoff F, Helmchen F. Resting microglial cells are highly
1081 dynamic surveillants of brain parenchyma in vivo. Science. 2005;308(5726):1314-8. Epub
1082 2005/04/16. doi: 10.1126/science.1110647. PubMed PMID: 15831717.

1083 23. Alvarez-Carbonell D, Ye F, Ramanath N, Garcia-Mesa Y, Knapp PE, Hauser KF,
1084 et al. Cross-talk between microglia and neurons regulates HIV latency. PLoS pathogens.
1085 2019;15(12):e1008249. Epub 2019/12/31. doi: 10.1371/journal.ppat.1008249. PubMed
1086 PMID: 31887215; PubMed Central PMCID: PMCPMC6953890.

1087 24. Smith LK, Kuhn TB, Chen J, Bamburg JR. HIV Associated Neurodegenerative
1088 Disorders: A New Perspective on the Role of Lipid Rafts in Gp120-Mediated
1089 Neurotoxicity. Current HIV research. 2018;16(4):258-69. Epub 2018/10/04. doi:
1090 10.2174/1570162X16666181003144740. PubMed PMID: 30280668; PubMed Central
1091 PMCID: PMCPMC6398609.

1092 25. Belichenko PV, Miklossy J, Celio MR. HIV-I induced destruction of neocortical
1093 extracellular matrix components in AIDS victims. Neurobiology of disease. 1997;4(3-
1094 4):301-10. Epub 1997/01/01. doi: 10.1006/nbdi.1997.0143. PubMed PMID: 9361307.

1095 26. Bagetta G, Corasaniti MT, Berliocchi L, Navarra M, Finazzi-Agro A, Nistico G. HIV-
1096 1 gp120 produces DNA fragmentation in the cerebral cortex of rat. Biochemical and
1097 biophysical research communications. 1995;211(1):130-6. Epub 1995/06/06. doi:
1098 10.1006/bbrc.1995.1787. PubMed PMID: 7779077.

1099 27. Marino J, Maubert ME, Mele AR, Spector C, Wigdahl B, Nonnemacher MR.
1100 Functional impact of HIV-1 Tat on cells of the CNS and its role in HAND. Cell Mol Life
1101 Sci. 2020;77(24):5079-99. Epub 2020/06/25. doi: 10.1007/s00018-020-03561-4. PubMed
1102 PMID: 32577796; PubMed Central PMCID: PMCPMC7674201.

1103 28. Minagar A, Shapshak P, Fujimura R, Ownby R, Heyes M, Eisdorfer C. The role of
1104 macrophage/microglia and astrocytes in the pathogenesis of three neurologic disorders:
1105 HIV-associated dementia, Alzheimer disease, and multiple sclerosis. J Neurol Sci.
1106 2002;202(1-2):13-23. Epub 2002/09/11. doi: 10.1016/s0022-510x(02)00207-1. PubMed
1107 PMID: 12220687.

1108 29. Galicia O, Sanchez-Alavez M, Mendez Diaz M, Navarro L, Prospero-Garcia O.
1109 [HIV glycoprotein 120: possible etiological agent of AIDS-associated dementia]. Rev
1110 Invest Clin. 2002;54(5):437-52. Epub 2003/02/18. PubMed PMID: 12587419.

30. Kaushik DK, Gupta M, Basu A. Microglial response to viral challenges: every silver lining comes with a cloud. Front Biosci (Landmark Ed). 2011;16:2187-205. Epub 2011/05/31. doi: 10.2741/3847. PubMed PMID: 21622170.

31. Periyasamy P, Thangaraj A, Bendi VS, Buch S. HIV-1 Tat-mediated microglial inflammation involves a novel miRNA-34a-NLRC5-NFkappaB signaling axis. Brain Behav Immun. 2019;80:227-37. Epub 2019/03/16. doi: 10.1016/j.bbi.2019.03.011. PubMed PMID: 30872089; PubMed Central PMCID: PMCPMC6660398.

32. Catani MV, Corasaniti MT, Navarra M, Nistico G, Finazzi-Agro A, Melino G. gp120 induces cell death in human neuroblastoma cells through the CXCR4 and CCR5 chemokine receptors. Journal of neurochemistry. 2000;74(6):2373-9. Epub 2000/05/23. doi: 10.1046/j.1471-4159.2000.0742373.x. PubMed PMID: 10820198.

33. Zhu Q, Song X, Zhou J, Wang Y, Xia J, Qian W, et al. Target of HIV-1 Envelope Glycoprotein gp120-Induced Hippocampal Neuron Damage: Role of Voltage-Gated K(+) Channel Kv2.1. Viral Immunol. 2015;28(9):495-503. Epub 2015/09/24. doi: 10.1089/vim.2015.0020. PubMed PMID: 26393286; PubMed Central PMCID: PMCPMC4642831.

34. Rom I, Deshmane SL, Mukerjee R, Khalili K, Amini S, Sawaya BE. HIV-1 Vpr deregulates calcium secretion in neural cells. Brain research. 2009;1275:81-6. Epub 2009/03/31. doi: 10.1016/j.brainres.2009.03.024. PubMed PMID: 19328187; PubMed Central PMCID: PMCPMC2692350.

35. Chompre G, Cruz E, Maldonado L, Rivera-Amill V, Porter JT, Noel RJ, Jr. Astrocytic expression of HIV-1 Nef impairs spatial and recognition memory. Neurobiology of disease. 2013;49:128-36. Epub 2012/08/29. doi: 10.1016/j.nbd.2012.08.007. PubMed PMID: 22926191; PubMed Central PMCID: PMCPMC3530662.

36. Alvarez-Carbonell D, Ye F, Ramanath N, Dobrowolski C, Karn J. The Glucocorticoid Receptor Is a Critical Regulator of HIV Latency in Human Microglial Cells. J Neuroimmune Pharmacol. 2018. Epub 2018/07/11. doi: 10.1007/s11481-018-9798-1. PubMed PMID: 29987742.

37. Garcia-Mesa Y, Jay TR, Checkley MA, Luttge B, Dobrowolski C, Valadkhan S, et al. Immortalization of primary microglia: a new platform to study HIV regulation in the central nervous system. J Neurovirol. 2017;23(1):47-66. Epub 2016/11/23. doi: 10.1007/s13365-016-0499-3. PubMed PMID: 27873219; PubMed Central PMCID: PMCPMC5329090.

38. Alvarez-Carbonell D, Garcia-Mesa Y, Milne S, Das B, Dobrowolski C, Rojas R, et al. Toll-like receptor 3 activation selectively reverses HIV latency in microglial cells. Retrovirology. 2017;14(1):9. Epub 2017/02/09. doi: 10.1186/s12977-017-0335-8. PubMed PMID: 28166799; PubMed Central PMCID: PMCPMC5294768.

39. Eilebrecht S, Le Douce V, Riclet R, Targat B, Hallay H, Van Driessche B, et al. HMGA1 recruits CTIP2-repressed P-TEFb to the HIV-1 and cellular target promoters.

1150 Nucleic Acids Res. 2014. Epub 2014/03/14. doi: 10.1093/nar/gku168. PubMed PMID:
1151 24623795.

1152 40. Cherrier T, Le Douce V, Eilebrecht S, Riclet R, Marban C, Dequiedt F, et al. CTIP2
1153 is a negative regulator of P-TEFb. Proc Natl Acad Sci U S A. 2013;110(31):12655-60.
1154 Epub 2013/07/16. doi: 10.1073/pnas.1220136110. PubMed PMID: 23852730; PubMed
1155 Central PMCID: PMC3732990.

1156 41. Van Lint C, Bouchat S, Marcello A. HIV-1 transcription and latency: an update.
1157 Retrovirology. 2013;10:67. Epub 2013/06/28. doi: 10.1186/1742-4690-10-67. PubMed
1158 PMID: 23803414; PubMed Central PMCID: PMC3699421.

1159 42. Marban C, Suzanne S, Dequiedt F, de Walque S, Redel L, Van Lint C, et al.
1160 Recruitment of chromatin-modifying enzymes by CTIP2 promotes HIV-1 transcriptional
1161 silencing. EMBO J. 2007;26(2):412-23. PubMed PMID: 17245431.

1162 43. Quivy V, Van Lint C. Diversity of acetylation targets and roles in transcriptional
1163 regulation: the human immunodeficiency virus type 1 promoter as a model system.
1164 Biochem Pharmacol. 2002;64:925-34.

1165 44. Van Lint C, Emiliani S, Ott M, Verdin E. Transcriptional activation and chromatin
1166 remodeling of the HIV-1 promoter in response to histone acetylation. EMBO J.
1167 1996;15(5):1112-20.

1168 45. Alvarez-Carbonell D, Ye F, Ramanath N, Dobrowolski C, Karn J. The
1169 Glucocorticoid Receptor Is a Critical Regulator of HIV Latency in Human Microglial Cells.
1170 Journal of neuroimmune pharmacology : the official journal of the Society on
1171 NeuroImmune Pharmacology. 2019;14(1):94-109. Epub 2018/07/11. doi:
1172 10.1007/s11481-018-9798-1. PubMed PMID: 29987742; PubMed Central PMCID:
1173 PMCPMC6394485.

1174 46. Zetterström RH, Solomin L, Mitsiadis T, Olson L, Perlmann T. Retinoid X receptor
1175 heterodimerization and developmental expression distinguish the orphan nuclear
1176 receptors NGFI-B, Nurr1, and Nor1. Mol Endocrinol. 1996;10(12):1656-66. Epub
1177 1996/12/01. doi: 10.1210/mend.10.12.8961274. PubMed PMID: 8961274.

1178 47. Saucedo-Cardenas O, Quintana-Hau JD, Le WD, Smidt MP, Cox JJ, De Mayo F,
1179 et al. Nurr1 is essential for the induction of the dopaminergic phenotype and the survival
1180 of ventral mesencephalic late dopaminergic precursor neurons. Proceedings of the
1181 National Academy of Sciences of the United States of America. 1998;95(7):4013-8. Epub
1182 1998/05/09. doi: 10.1073/pnas.95.7.4013. PubMed PMID: 9520484; PubMed Central
1183 PMCID: PMCPMC19954.

1184 48. Sonntag KC, Simantov R, Kim KS, Isacson O. Temporally induced Nurr1 can
1185 induce a non-neuronal dopaminergic cell type in embryonic stem cell differentiation. The
1186 European journal of neuroscience. 2004;19(5):1141-52. Epub 2004/03/16. doi:
1187 10.1111/j.1460-9568.2004.03204.x. PubMed PMID: 15016073; PubMed Central PMCID:
1188 PMCPMC2614072.

1189 49. Eells JB, Wilcots J, Sisk S, Guo-Ross SX. NR4A gene expression is dynamically
1190 regulated in the ventral tegmental area dopamine neurons and is related to expression of
1191 dopamine neurotransmission genes. J Mol Neurosci. 2012;46(3):545-53. Epub
1192 2011/09/21. doi: 10.1007/s12031-011-9642-z. PubMed PMID: 21932041; PubMed
1193 Central PMCID: PMCPMC3280384.

1194 50. Saijo K, Winner B, Carson CT, Collier JG, Boyer L, Rosenfeld MG, et al. A
1195 Nurr1/CoREST pathway in microglia and astrocytes protects dopaminergic neurons from
1196 inflammation-induced death. Cell. 2009;137(1):47-59. Epub 2009/04/07. doi:
1197 10.1016/j.cell.2009.01.038. PubMed PMID: 19345186; PubMed Central PMCID:
1198 PMC2754279.

1199 51. Jeon SG, Yoo A, Chun DW, Hong SB, Chung H, Kim JI, et al. The Critical Role of
1200 Nurr1 as a Mediator and Therapeutic Target in Alzheimer's Disease-related
1201 Pathogenesis. Aging Dis. 2020;11(3):705-24. Epub 2020/06/04. doi:
1202 10.14336/AD.2019.0718. PubMed PMID: 32489714; PubMed Central PMCID:
1203 PMCPMC7220289.

1204 52. Kandil EA, Sayed RH, Ahmed LA, Abd El Fattah MA, El-Sayeh BM. Modulatory
1205 Role of Nurr1 Activation and Thrombin Inhibition in the Neuroprotective Effects of
1206 Dabigatran Etexilate in Rotenone-Induced Parkinson's Disease in Rats. Molecular
1207 neurobiology. 2018;55(5):4078-89. Epub 2017/06/07. doi: 10.1007/s12035-017-0636-x.
1208 PubMed PMID: 28585189.

1209 53. Smith GA, Rocha EM, Rooney T, Barneoud P, McLean JR, Beagan J, et al. A
1210 Nurr1 agonist causes neuroprotection in a Parkinson's disease lesion model primed with
1211 the toll-like receptor 3 dsRNA inflammatory stimulant poly(I:C). PloS one.
1212 2015;10(3):e0121072. Epub 2015/03/31. doi: 10.1371/journal.pone.0121072. PubMed
1213 PMID: 25815475; PubMed Central PMCID: PMCPMC4376720 This does not alter the
1214 authors' adherence to PLOS ONE policies on sharing data and materials.

1215 54. Liu W, Gao Y, Chang N. Nurr1 overexpression exerts neuroprotective and anti-
1216 inflammatory roles via down-regulating CCL2 expression in both in vivo and in vitro
1217 Parkinson's disease models. Biochemical and biophysical research communications.
1218 2017;482(4):1312-9. Epub 2016/12/13. doi: 10.1016/j.bbrc.2016.12.034. PubMed PMID:
1219 27940361.

1220 55. Moon M, Jung ES, Jeon SG, Cha MY, Jang Y, Kim W, et al. Nurr1 (NR4A2)
1221 regulates Alzheimer's disease-related pathogenesis and cognitive function in the 5XFAD
1222 mouse model. Aging Cell. 2019;18(1):e12866. Epub 2018/12/06. doi:
1223 10.1111/acel.12866. PubMed PMID: 30515963; PubMed Central PMCID:
1224 PMCPMC6351845.

1225 56. Li X, Tjalkens RB, Shrestha R, Safe S. Structure-dependent activation of gene
1226 expression by bis-indole and quinoline-derived activators of nuclear receptor 4A2. Chem
1227 Biol Drug Des. 2019;94(4):1711-20. Epub 2019/05/19. doi: 10.1111/cbdd.13564. PubMed
1228 PMID: 31102570; PubMed Central PMCID: PMCPMC6791730.

1229 57. Das B, Dobrowolski C, Luttge B, Valadkhan S, Chomont N, Johnston R, et al.
1230 Estrogen Receptor α (ESR1) is a key regulator of HIV-1 latency that imparts gender-
1231 specific restrictions on the latent reservoir
1232 Proc Natl Acad Sci U S A. 2018;In press.

1233 58. Li Q, Karim AF, Ding X, Das B, Dobrowolski C, Gibson RM, et al. Novel high
1234 throughput pooled shRNA screening identifies NQO1 as a potential drug target for host
1235 directed therapy for tuberculosis. Sci Rep. 2016;6:27566. Epub 2016/06/15. doi:
1236 10.1038/srep27566. PubMed PMID: 27297123; PubMed Central PMCID:
1237 PMCPMC4906352.

1238 59. Wires ES, Alvarez D, Dobrowolski C, Wang Y, Morales M, Karn J, et al.
1239 Methamphetamine activates nuclear factor kappa-light-chain-enhancer of activated B
1240 cells (NF-kappaB) and induces human immunodeficiency virus (HIV) transcription in
1241 human microglial cells. J Neurovirol. 2012;18(5):400-10. Epub 2012/05/24. doi:
1242 10.1007/s13365-012-0103-4. PubMed PMID: 22618514; PubMed Central PMCID:
1243 PMC3469781.

1244 60. Shtutman M, Maliyekkel A, Shao Y, Carmack CS, Baig M, Warholic N, et al.
1245 Function-based gene identification using enzymatically generated normalized shRNA
1246 library and massive parallel sequencing. Proc Natl Acad Sci U S A. 2010;107(16):7377-
1247 82. Epub 2010/04/07. doi: 1003055107 [pii]
1248 10.1073/pnas.1003055107. PubMed PMID: 20368428; PubMed Central PMCID:
1249 PMC2867740.

1250 61. Sims D, Mendes-Pereira AM, Frankum J, Burgess D, Cerone MA, Lombardelli C,
1251 et al. High-throughput RNA interference screening using pooled shRNA libraries and next
1252 generation sequencing. Genome Biol. 2011;12(10):R104. Epub 2011/10/25. doi:
1253 10.1186/gb-2011-12-10-r104. PubMed PMID: 22018332; PubMed Central PMCID:
1254 PMC3333774.

1255 62. Llewellyn GN, Alvarez-Carbonell D, Chateau M, Karn J, Cannon PM. HIV-1
1256 infection of microglial cells in a reconstituted humanized mouse model and identification
1257 of compounds that selectively reverse HIV latency. Journal of neurovirology. 2017. Epub
1258 2017/12/20. doi: 10.1007/s13365-017-0604-2. PubMed PMID: 29256041.

1259 63. Das B, Dobrowolski C, Luttge B, Valadkhan S, Chomont N, Johnston R, et al.
1260 Estrogen receptor-1 is a key regulator of HIV-1 latency that imparts gender-specific
1261 restrictions on the latent reservoir. Proc Natl Acad Sci U S A. 2018;115(33):E7795-e804.
1262 Epub 2018/08/01. doi: 10.1073/pnas.1803468115. PubMed PMID: 30061382; PubMed
1263 Central PMCID: PMCPmc6099847.

1264 64. Wang J, Bi W, Zhao W, Varghese M, Koch RJ, Walker RH, et al. Selective brain
1265 penetrable Nurr1 transactivator for treating Parkinson's disease. Oncotarget.
1266 2016;7(7):7469-79. Epub 2016/02/11. doi: 10.18632/oncotarget.7191. PubMed PMID:
1267 26862735; PubMed Central PMCID: PMCPMC4884932.

65. Dong J, Li S, Mo JL, Cai HB, Le WD. Nurr1-Based Therapies for Parkinson's Disease. CNS Neurosci Ther. 2016;22(5):351-9. Epub 2016/03/26. doi: 10.1111/cns.12536. PubMed PMID: 27012974; PubMed Central PMCID: PMCPMC4833611.

66. Chen XX, Qian Y, Wang XP, Tang ZW, Xu JT, Lin H, et al. Nurr1 promotes neurogenesis of dopaminergic neuron and represses inflammatory factors in the transwell coculture system of neural stem cells and microglia. CNS neuroscience & therapeutics. 2018;24(9):790-800. Epub 2018/02/17. doi: 10.1111/cns.12825. PubMed PMID: 29450981; PubMed Central PMCID: PMCPMC6489950.

67. Kim CH, Han BS, Moon J, Kim DJ, Shin J, Rajan S, et al. Nuclear receptor Nurr1 agonists enhance its dual functions and improve behavioral deficits in an animal model of Parkinson's disease. Proceedings of the National Academy of Sciences of the United States of America. 2015;112(28):8756-61. Epub 2015/07/01. doi: 10.1073/pnas.1509742112. PubMed PMID: 26124091; PubMed Central PMCID: PMCPMC4507186.

68. Wansa KD, Harris JM, Yan G, Ordentlich P, Muscat GE. The AF-1 domain of the orphan nuclear receptor NOR-1 mediates trans-activation, coactivator recruitment, and activation by the purine anti-metabolite 6-mercaptopurine. The Journal of biological chemistry. 2003;278(27):24776-90. Epub 2003/04/24. doi: 10.1074/jbc.M300088200. PubMed PMID: 12709428.

69. Ordentlich P, Yan Y, Zhou S, Heyman RA. Identification of the antineoplastic agent 6-mercaptopurine as an activator of the orphan nuclear hormone receptor Nurr1. The Journal of biological chemistry. 2003;278(27):24791-9. Epub 2003/04/24. doi: 10.1074/jbc.M302167200. PubMed PMID: 12709433.

70. Rodriguez-Calvo R, Ferran B, Alonso J, Marti-Pamies I, Aguilo S, Calvayrac O, et al. NR4A receptors up-regulate the antiproteinase alpha-2 macroglobulin (A2M) and modulate MMP-2 and MMP-9 in vascular smooth muscle cells. Thromb Haemost. 2015;113(6):1323-34. Epub 2015/03/27. doi: 10.1160/TH14-07-0645. PubMed PMID: 25809189.

71. Bozzelli PL, Caccavano A, Avdoshina V, Mocchetti I, Wu JY, Conant K. Increased matrix metalloproteinase levels and perineuronal net proteolysis in the HIV-infected brain; relevance to altered neuronal population dynamics. Experimental neurology. 2020;323:113077. Epub 2019/11/05. doi: 10.1016/j.expneurol.2019.113077. PubMed PMID: 31678140.

72. van Neerven S, Kampmann E, Mey J. RAR/RXR and PPAR/RXR signaling in neurological and psychiatric diseases. Progress in neurobiology. 2008;85(4):433-51. Epub 2008/06/17. doi: 10.1016/j.pneurobio.2008.04.006. PubMed PMID: 18554773.

73. Zuo Y, Huang L, Enkhjargal B, Xu W, Umut O, Travis ZD, et al. Activation of retinoid X receptor by bexarotene attenuates neuroinflammation via PPARγ/SIRT6/FoxO3a pathway after subarachnoid hemorrhage in rats. J

1308 Neuroinflammation. 2019;16(1):47. Epub 2019/02/23. doi: 10.1186/s12974-019-1432-5.
1309 PubMed PMID: 30791908; PubMed Central PMCID: PMCPMC6385420.

1310 74. Boehm-Cagan A, Michaelson DM. Reversal of apoE4-driven brain pathology and
1311 behavioral deficits by bexarotene. The Journal of neuroscience : the official journal of the
1312 Society for Neuroscience. 2014;34(21):7293-301. Epub 2014/05/23. doi:
1313 10.1523/JNEUROSCI.5198-13.2014. PubMed PMID: 24849361; PubMed Central
1314 PMCID: PMCPMC6608187.

1315 75. Mariani MM, Malm T, Lamb R, Jay TR, Neilson L, Casali B, et al. Neuronally-
1316 directed effects of RXR activation in a mouse model of Alzheimer's disease. Scientific
1317 reports. 2017;7:42270. Epub 2017/02/17. doi: 10.1038/srep42270. PubMed PMID:
1318 28205585; PubMed Central PMCID: PMCPMC5311933.

1319 76. Ghosal K, Haag M, Verghese PB, West T, Veenstra T, Braunstein JB, et al. A
1320 randomized controlled study to evaluate the effect of bexarotene on amyloid-beta and
1321 apolipoprotein E metabolism in healthy subjects. Alzheimer's & dementia (New York, N
1322 Y). 2016;2(2):110-20. Epub 2016/06/17. doi: 10.1016/j.trci.2016.06.001. PubMed PMID:
1323 29067298; PubMed Central PMCID: PMCPMC5644280.

1324 77. Casali BT, Reed-Geaghan EG, Landreth GE. Nuclear receptor agonist-driven
1325 modification of inflammation and amyloid pathology enhances and sustains cognitive
1326 improvements in a mouse model of Alzheimer's disease. J Neuroinflammation.
1327 2018;15(1):43. Epub 2018/02/17. doi: 10.1186/s12974-018-1091-y. PubMed PMID:
1328 29448961; PubMed Central PMCID: PMCPMC5815248.

1329 78. De Miranda BR, Popichak KA, Hammond SL, Jorgensen BA, Phillips AT, Safe S,
1330 et al. The Nurr1 Activator 1,1-Bis(3'-Indolyl)-1-(p-Chlorophenyl)Methane Blocks
1331 Inflammatory Gene Expression in BV-2 Microglial Cells by Inhibiting Nuclear Factor
1332 kappaB. Mol Pharmacol. 2015;87(6):1021-34. Epub 2015/04/11. doi:
1333 10.1124/mol.114.095398. PubMed PMID: 25858541; PubMed Central PMCID:
1334 PMCPMC4429718.

1335 79. Tsai MC, Manor O, Wan Y, Mosammaparast N, Wang JK, Lan F, et al. Long
1336 noncoding RNA as modular scaffold of histone modification complexes. Science.
1337 2010;329(5992):689-93. Epub 2010/07/10. doi: 10.1126/science.1192002. PubMed
1338 PMID: 20616235; PubMed Central PMCID: PMC2967777.

1339 80. Gu H, Liang Y, Mandel G, Roizman B. Components of the REST/CoREST/histone
1340 deacetylase repressor complex are disrupted, modified, and translocated in HSV-1-
1341 infected cells. Proceedings of the National Academy of Sciences of the United States of
1342 America. 2005;102(21):7571-6. Epub 2005/05/18. doi: 10.1073/pnas.0502658102.
1343 PubMed PMID: 15897453; PubMed Central PMCID: PMCPMC1140450.

1344 81. Vallat-Decouvelaere AV, Gray F, Chretien F, Le Pavec G, Dormont D, Gras G.
1345 [Neurotoxicity and neuroprotection, two aspects of microglial activation in human
1346 immunodeficiency virus (HIV) infection]. Ann Pathol. 2004;24(1):31-44. Epub 2004/06/12.
1347 doi: 10.1016/s0242-6498(04)93895-3. PubMed PMID: 15192535.

82. Thangaraj A, Chivero ET, Tripathi A, Singh S, Niu F, Guo ML, et al. HIV TAT-mediated microglial senescence: Role of SIRT3-dependent mitochondrial oxidative stress. Redox Biol. 2021;40:101843. Epub 2021/01/02. doi: 10.1016/j.redox.2020.101843. PubMed PMID: 33385630; PubMed Central PMCID: PMCPMC7779826.

83. Silverstein PS, Shah A, Weemhoff J, Kumar S, Singh DP, Kumar A. HIV-1 gp120 and drugs of abuse: interactions in the central nervous system. Current HIV research. 2012;10(5):369-83. Epub 2012/05/18. doi: 10.2174/157016212802138724. PubMed PMID: 22591361; PubMed Central PMCID: PMCPMC4086306.

84. Narasipura SD, Kim S, Al-Harthi L. Epigenetic regulation of HIV-1 latency in astrocytes. Journal of virology. 2014;88(5):3031-8. Epub 2013/12/20. doi: 10.1128/JVI.03333-13. PubMed PMID: 24352441; PubMed Central PMCID: PMCPMC3958059.

85. Shirazi J, Shah S, Sagar D, Nonnemacher MR, Wigdahl B, Khan ZK, et al. Epigenetics, drugs of abuse, and the retroviral promoter. Journal of neuroimmune pharmacology : the official journal of the Society on NeuroImmune Pharmacology. 2013;8(5):1181-96. Epub 2013/11/13. doi: 10.1007/s11481-013-9508-y. PubMed PMID: 24218017; PubMed Central PMCID: PMCPMC3878082.

86. Rohr O, Aunis D, Schaeffer E. COUP-TF and Sp1 interact and cooperate in the transcriptional activation of the human immunodeficiency virus type 1 long terminal repeat in human microglial cells. The Journal of biological chemistry. 1997;272(49):31149-55. Epub 1998/01/10. doi: 10.1074/jbc.272.49.31149. PubMed PMID: 9388268.

87. Marban C, Redel L, Suzanne S, Van Lint C, Lecestre D, Chasserot-Golaz S, et al. COUP-TF interacting protein 2 represses the initial phase of HIV-1 gene transcription in human microglial cells. Nucleic Acids Res. 2005;33(7):2318-31. Epub 2005/04/26. doi: 10.1093/nar/gki529. PubMed PMID: 15849318; PubMed Central PMCID: PMCPMC1084325.

88. Marban C, Suzanne S, Dequiedt F, de Walque S, Redel L, Van Lint C, et al. Recruitment of chromatin-modifying enzymes by CTIP2 promotes HIV-1 transcriptional silencing. The EMBO journal. 2007;26(2):412-23. Epub 2007/01/25. doi: 10.1038/sj.emboj.7601516. PubMed PMID: 17245431; PubMed Central PMCID: PMCPMC1783449.

89. Le Douce V, Colin L, Redel L, Cherrier T, Herbein G, Aunis D, et al. LSD1 cooperates with CTIP2 to promote HIV-1 transcriptional silencing. Nucleic Acids Res. 2012;40(5):1904-15. Epub 2011/11/10. doi: 10.1093/nar/gkr857. PubMed PMID: 22067449; PubMed Central PMCID: PMCPMC3300010.

90. Cherrier T, Le Douce V, Eilebrecht S, Riclet R, Marban C, Dequiedt F, et al. CTIP2 is a negative regulator of P-TEFb. Proceedings of the National Academy of Sciences of the United States of America. 2013;110(31):12655-60. Epub 2013/07/16. doi:

1387 10.1073/pnas.1220136110. PubMed PMID: 23852730; PubMed Central PMCID:
1388 PMCPMC3732990.

1389 91. De Bosscher K, Desmet SJ, Clarisse D, Estebanez-Perpina E, Brunsveld L.
1390 Nuclear receptor crosstalk - defining the mechanisms for therapeutic innovation. Nat Rev
1391 Endocrinol. 2020;16(7):363-77. Epub 2020/04/19. doi: 10.1038/s41574-020-0349-5.
1392 PubMed PMID: 32303708.

1393 92. Kurakula K, Koenis DS, van Tiel CM, de Vries CJ. NR4A nuclear receptors are
1394 orphans but not lonesome. Biochimica et biophysica acta. 2014;1843(11):2543-55. Epub
1395 2014/07/01. doi: 10.1016/j.bbamcr.2014.06.010. PubMed PMID: 24975497.

1396 93. Wallen-Mackenzie A, Mata de Urquiza A, Petersson S, Rodriguez FJ, Friling S,
1397 Wagner J, et al. Nurr1-RXR heterodimers mediate RXR ligand-induced signaling in
1398 neuronal cells. Genes Dev. 2003;17(24):3036-47. Epub 2003/12/19. doi:
1399 10.1101/gad.276003. PubMed PMID: 14681209; PubMed Central PMCID:
1400 PMCPMC305256.

1401 94. Kadkhodaei B, Ito T, Joodmardi E, Mattsson B, Rouillard C, Carta M, et al. Nurr1
1402 is required for maintenance of maturing and adult midbrain dopamine neurons. The
1403 Journal of neuroscience : the official journal of the Society for Neuroscience.
1404 2009;29(50):15923-32. Epub 2009/12/18. doi: 10.1523/JNEUROSCI.3910-09.2009.
1405 PubMed PMID: 20016108; PubMed Central PMCID: PMCPMC6666174.

1406 95. Tornqvist N, Hermanson E, Perlmann T, Stromberg I. Generation of tyrosine
1407 hydroxylase-immunoreactive neurons in ventral mesencephalic tissue of Nurr1 deficient
1408 mice. Brain Res Dev Brain Res. 2002;133(1):37-47. Epub 2002/02/19. doi:
1409 10.1016/s0165-3806(01)00317-0. PubMed PMID: 11850062.

1410 96. Decressac M, Volakakis N, Bjorklund A, Perlmann T. NURR1 in Parkinson
1411 disease--from pathogenesis to therapeutic potential. Nature reviews Neurology.
1412 2013;9(11):629-36. Epub 2013/10/16. doi: 10.1038/nrneurol.2013.209. PubMed PMID:
1413 24126627.

1414 97. Liu H, Wei L, Tao Q, Deng H, Ming M, Xu P, et al. Decreased NURR1 and PITX3
1415 gene expression in Chinese patients with Parkinson's disease. Eur J Neurol.
1416 2012;19(6):870-5. Epub 2012/02/09. doi: 10.1111/j.1468-1331.2011.03644.x. PubMed
1417 PMID: 22309633.

1418 98. Bensinger SJ, Tontonoz P. A Nurr1 pathway for neuroprotection. Cell.
1419 2009;137(1):26-8. Epub 2009/04/07. doi: 10.1016/j.cell.2009.03.024. PubMed PMID:
1420 19345183.

1421 99. Spathis AD, Asvos X, Ziavra D, Karampelas T, Topouzis S, Cournia Z, et al.
1422 Nurr1:RXRalpha heterodimer activation as monotherapy for Parkinson's disease.
1423 Proceedings of the National Academy of Sciences of the United States of America.
1424 2017;114(15):3999-4004. Epub 2017/03/30. doi: 10.1073/pnas.1616874114. PubMed
1425 PMID: 28348207; PubMed Central PMCID: PMCPMC5393203.

1426 100. Edison P. Neuroinflammation, microglial activation, and glucose metabolism in
1427 neurodegenerative diseases. Int Rev Neurobiol. 2020;154:325-44. Epub 2020/08/03. doi:
1428 10.1016/bs.irn.2020.03.017. PubMed PMID: 32739010.

1429 101. Purisai MG, McCormack AL, Cumine S, Li J, Isla MZ, Di Monte DA. Microglial
1430 activation as a priming event leading to paraquat-induced dopaminergic cell
1431 degeneration. Neurobiology of disease. 2007;25(2):392-400. Epub 2006/12/15. doi:
1432 10.1016/j.nbd.2006.10.008. PubMed PMID: 17166727; PubMed Central PMCID:
1433 PMCPMC2001246.

1434 102. Spudich SS, Ances BM. Neurologic complications of HIV infection. Topics in
1435 antiviral medicine. 2012;20(2):41-7. Epub 2012/06/20. PubMed PMID: 22710906;
1436 PubMed Central PMCID: PMCPMC6148861.

1437 103. Zhang J, He H, Qiao Y, Zhou T, He H, Yi S, et al. Priming of microglia with IFN-
1438 gamma impairs adult hippocampal neurogenesis and leads to depression-like behaviors
1439 and cognitive defects. Glia. 2020. Epub 2020/07/12. doi: 10.1002/glia.23878. PubMed
1440 PMID: 32652855.

1441 104. Meda L, Cassatella MA, Szendrei GI, Otvos L, Jr., Baron P, Villalba M, et al.
1442 Activation of microglial cells by beta-amyloid protein and interferon-gamma. Nature.
1443 1995;374(6523):647-50. Epub 1995/04/13. doi: 10.1038/374647a0. PubMed PMID:
1444 7715705.

1445 105. Chao CC, Hu S, Molitor TW, Shaskan EG, Peterson PK. Activated microglia
1446 mediate neuronal cell injury via a nitric oxide mechanism. Journal of immunology
1447 (Baltimore, Md : 1950). 1992;149(8):2736-41. Epub 1992/10/15. PubMed PMID:
1448 1383325.

1449 106. Hwang IK, Choi JH, Nam SM, Park OK, Yoo DY, Kim W, et al. Activation of
1450 microglia and induction of pro-inflammatory cytokines in the hippocampus of type 2
1451 diabetic rats. Neurol Res. 2014;36(9):824-32. Epub 2014/02/28. doi:
1452 10.1179/1743132814Y.0000000330. PubMed PMID: 24571083.

1453 107. Shytaj IL, Procopio FA, Tarek M, Carlon-Andres I, Tang HY, Goldman AR, et al.
1454 Glycolysis downregulation is a hallmark of HIV-1 latency and sensitizes infected cells to
1455 oxidative stress. EMBO Mol Med. 2021;13(8):e13901. Epub 2021/07/22. doi:
1456 10.15252/emmm.202013901. PubMed PMID: 34289240; PubMed Central PMCID:
1457 PMCPMC8350904.

1458 108. Jakaria M, Haque ME, Cho DY, Azam S, Kim IS, Choi DK. Molecular Insights into
1459 NR4A2(Nurr1): an Emerging Target for Neuroprotective Therapy Against
1460 Neuroinflammation and Neuronal Cell Death. Molecular neurobiology. 2019;56(8):5799-
1461 814. Epub 2019/01/27. doi: 10.1007/s12035-019-1487-4. PubMed PMID: 30684217.

1462 109. Miguel-Escalada I, Bonas-Guarch S, Cebola I, Ponsa-Cobas J, Mendieta-Esteban
1463 J, Atla G, et al. Human pancreatic islet three-dimensional chromatin architecture provides
1464 insights into the genetics of type 2 diabetes. Nat Genet. 2019;51(7):1137-48. Epub

2019/06/30. doi: 10.1038/s41588-019-0457-0. PubMed PMID: 31253982; PubMed Central PMCID: PMCPMC6640048.

110. Friedman J, Cho WK, Chu CK, Keedy KS, Archin NM, Margolis DM, et al. Epigenetic silencing of HIV-1 by the histone H3 lysine 27 methyltransferase enhancer of Zeste 2. J Virol. 2011;85(17):9078-89. Epub 2011/07/01. doi: 10.1128/jvi.00836-11. PubMed PMID: 21715480; PubMed Central PMCID: PMCPmc3165831.

111. Afgan E, Baker D, van den Beek M, Blankenberg D, Bouvier D, Cech M, et al. The Galaxy platform for accessible, reproducible and collaborative biomedical analyses: 2016 update. Nucleic Acids Res. 2016;44(W1):W3-W10. Epub 2016/05/04. doi: 10.1093/nar/gkw343. PubMed PMID: 27137889; PubMed Central PMCID: PMCPMC4987906.

112. Langmead B, Trapnell C, Pop M, Salzberg SL. Ultrafast and memory-efficient alignment of short DNA sequences to the human genome. Genome Biol. 2009;10(3):R25. Epub 2009/03/06. doi: 10.1186/gb-2009-10-3-r25. PubMed PMID: 19261174; PubMed Central PMCID: PMCPMC2690996.

113. Langmead B, Salzberg SL. Fast gapped-read alignment with Bowtie 2. Nat Methods. 2012;9(4):357-9. Epub 2012/03/06. doi: 10.1038/nmeth.1923. PubMed PMID: 22388286; PubMed Central PMCID: PMCPMC3322381.

114. Ramirez F, Ryan DP, Gruning B, Bhardwaj V, Kilpert F, Richter AS, et al. deepTools2: a next generation web server for deep-sequencing data analysis. Nucleic Acids Res. 2016;44(W1):W160-5. Epub 2016/04/16. doi: 10.1093/nar/gkw257. PubMed PMID: 27079975; PubMed Central PMCID: PMCPMC4987876.

115. Dobin A, Gingeras TR. Mapping RNA-seq Reads with STAR. Curr Protoc Bioinformatics. 2015;51:11 4 1- 4 9. Epub 2015/09/04. doi: 10.1002/0471250953.bi1114s51. PubMed PMID: 26334920; PubMed Central PMCID: PMCPMC4631051.

116. Anders S, Pyl PT, Huber W. HTSeq--a Python framework to work with high-throughput sequencing data. Bioinformatics. 2015;31(2):166-9. Epub 2014/09/28. doi: 10.1093/bioinformatics/btu638. PubMed PMID: 25260700; PubMed Central PMCID: PMCPMC4287950.

117. Bray NL, Pimentel H, Melsted P, Pachter L. Near-optimal probabilistic RNA-seq quantification. Nat Biotechnol. 2016;34(5):525-7. Epub 2016/04/05. doi: 10.1038/nbt.3519. PubMed PMID: 27043002.

118. Robinson MD, McCarthy DJ, Smyth GK. edgeR: a Bioconductor package for differential expression analysis of digital gene expression data. Bioinformatics. 2010;26(1):139-40. Epub 2009/11/17. doi: 10.1093/bioinformatics/btp616. PubMed PMID: 19910308; PubMed Central PMCID: PMCPMC2796818.

119. Satija R, Farrell JA, Gennert D, Schier AF, Regev A. Spatial reconstruction of single-cell gene expression data. Nat Biotechnol. 2015;33(5):495-502. Epub 2015/04/14. doi: 10.1038/nbt.3192. PubMed PMID: 25867923; PubMed Central PMCID: PMCPMC4430369.

120. Kim YK, Bourgeois CF, Pearson R, Tyagi M, West MJ, Wong J, et al. Recruitment of TFIIH to the HIV LTR is a rate-limiting step in the emergence of HIV from latency. The EMBO journal. 2006;25(15):3596-604. Epub 2006/07/29. doi: 10.1038/sj.emboj.7601248. PubMed PMID: 16874302; PubMed Central PMCID: PMCPMC1538560.

A

Proviral HIV Structure

B

Experimental work flow

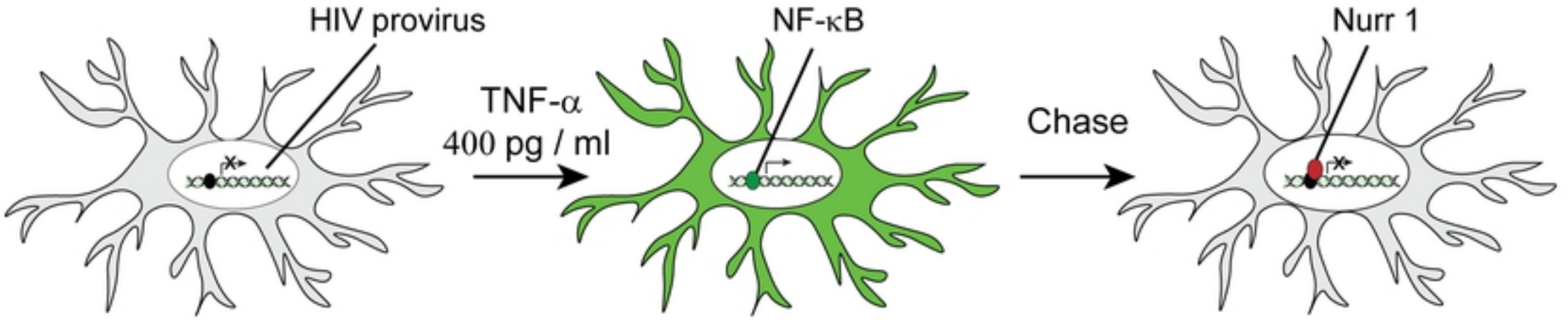

Latently infected microglia cell **Reactivated microglia cell (M1)** **Silenced microglia cell**

C

Reactivation and subsequent silencing of active HIV in hμglia cells (HC69)

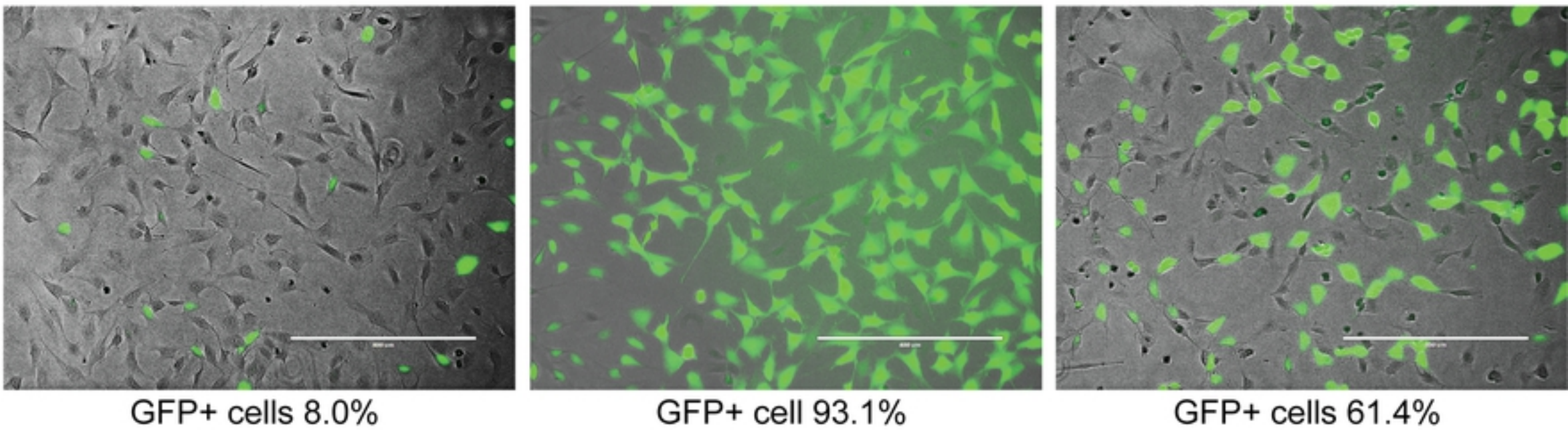

Figure 1

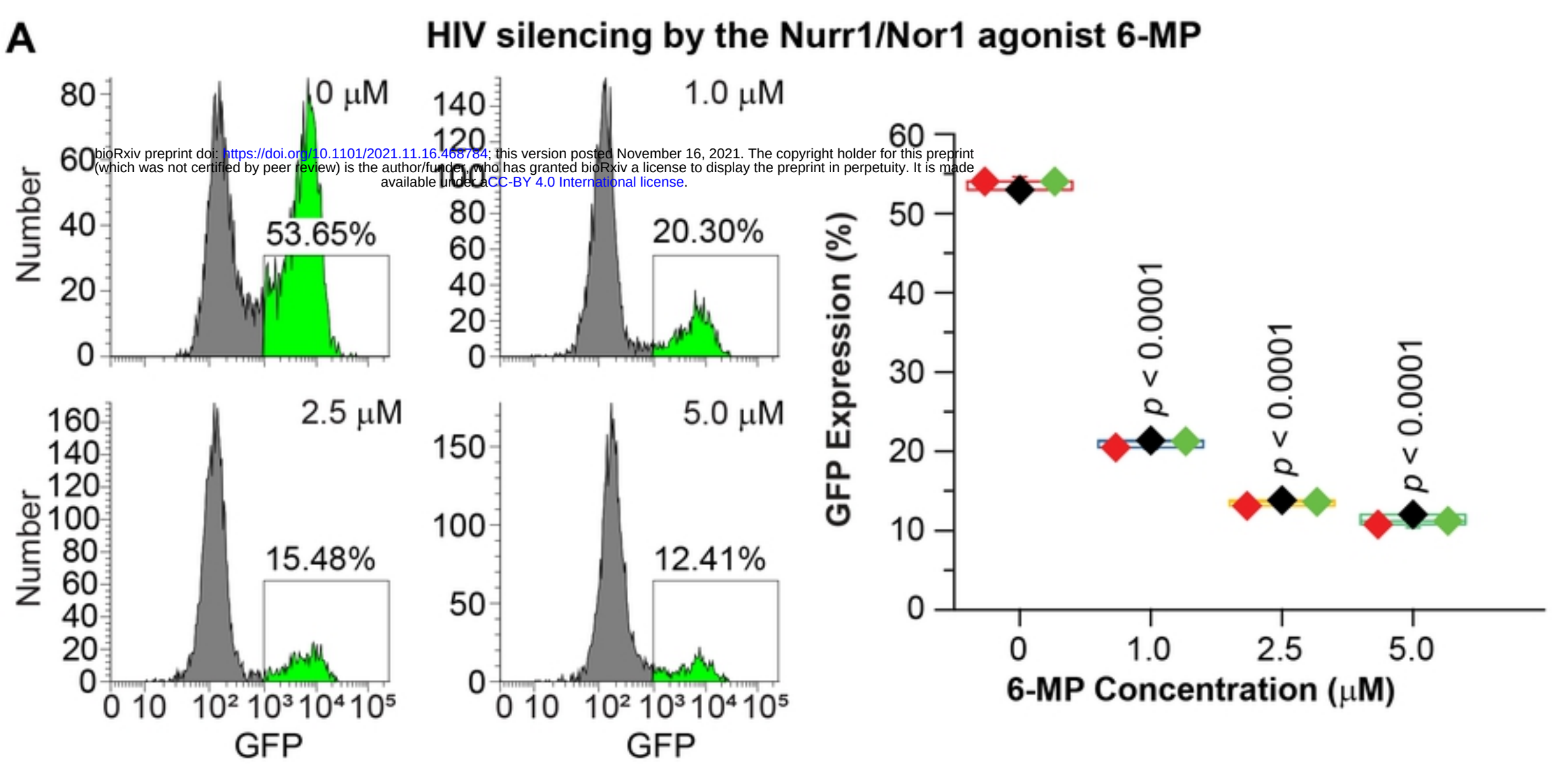

Figure 2

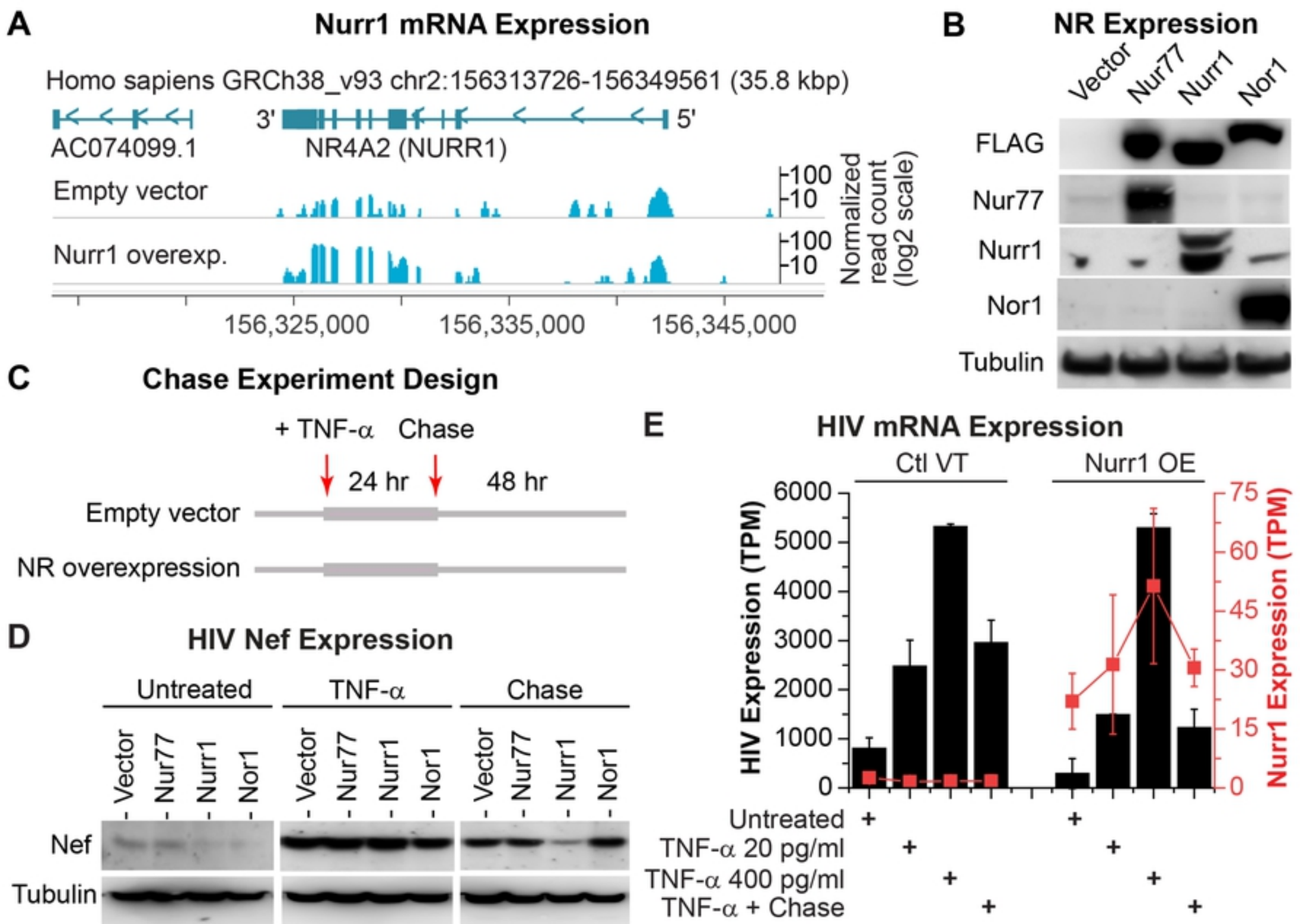
A
Nurr1 mRNA Expression
Homo sapiens GRCh38_v93 chr2:156313726-156349561 (35.8 kbp)
3'
5'
AC074099.1
NR4A2 (NURR1)
Empty vector
Nurr1 overexp.
100
10
100
10
Normalized read count (log2 scale)
156,325,000
156,335,000
156,345,000
B
NR Expression
Vector
Nur77
Nurr1
Nor1
FLAG
Nur77
Nurr1
Nor1
Tubulin
C
Chase Experiment Design
+ TNF-α
Chase
24 hr
48 hr
Empty vector
NR overexpression
D
HIV Nef Expression
Untreated
TNF-α
Chase
Vector
Nur77
Nurr1
Nor1
Nef
Tubulin
E
HIV mRNA Expression
Ctl VT
Nurr1 OE
HIV Expression (TPM)
6000
5000
4000
3000
2000
1000
0
75
60
45
30
15
0
Nurr1 Expression (TPM)
Untreated
TNF-α 20 pg/ml
TNF-α 400 pg/ml
TNF-α + Chase

Figure 3

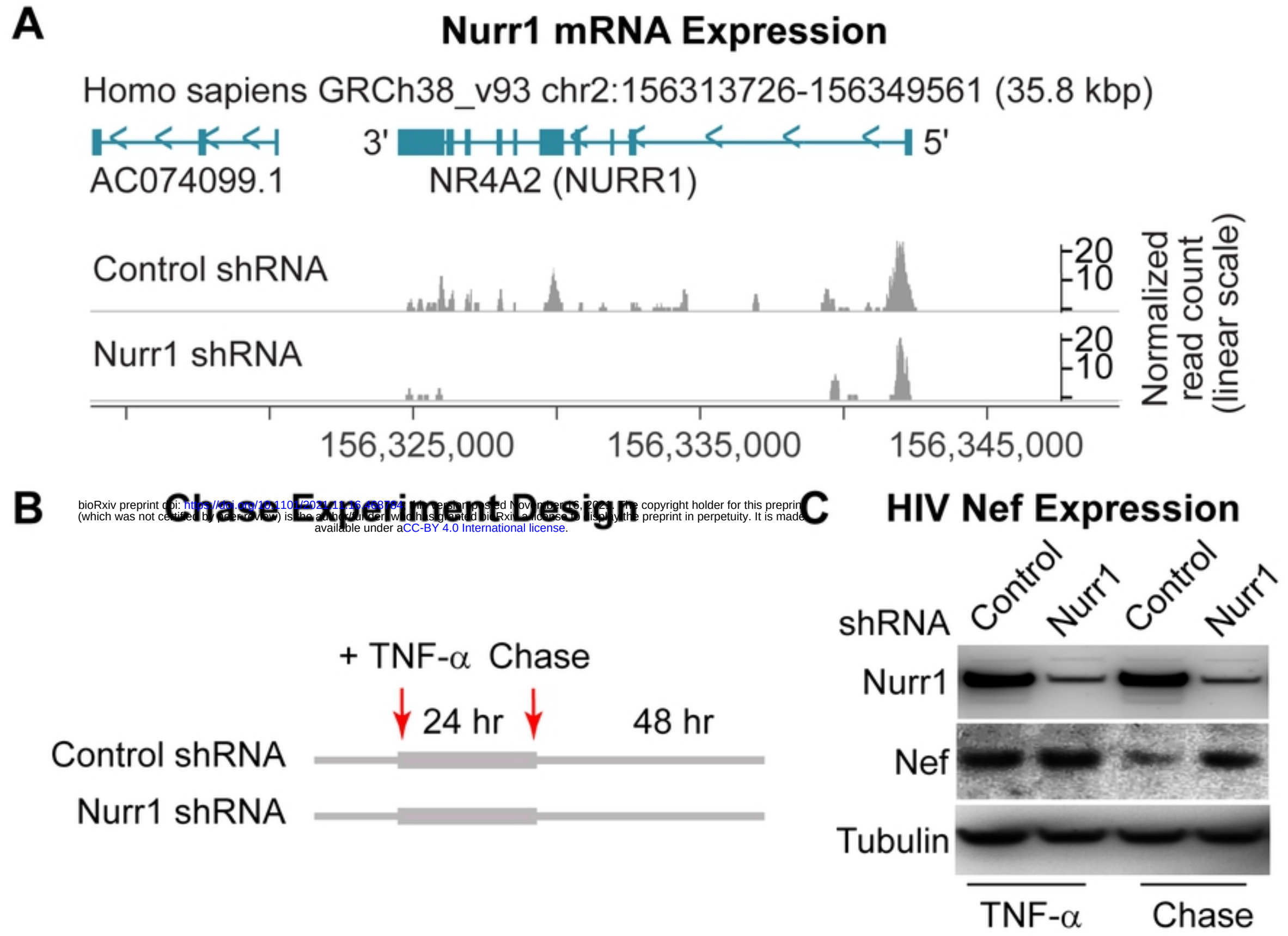

Figure 4

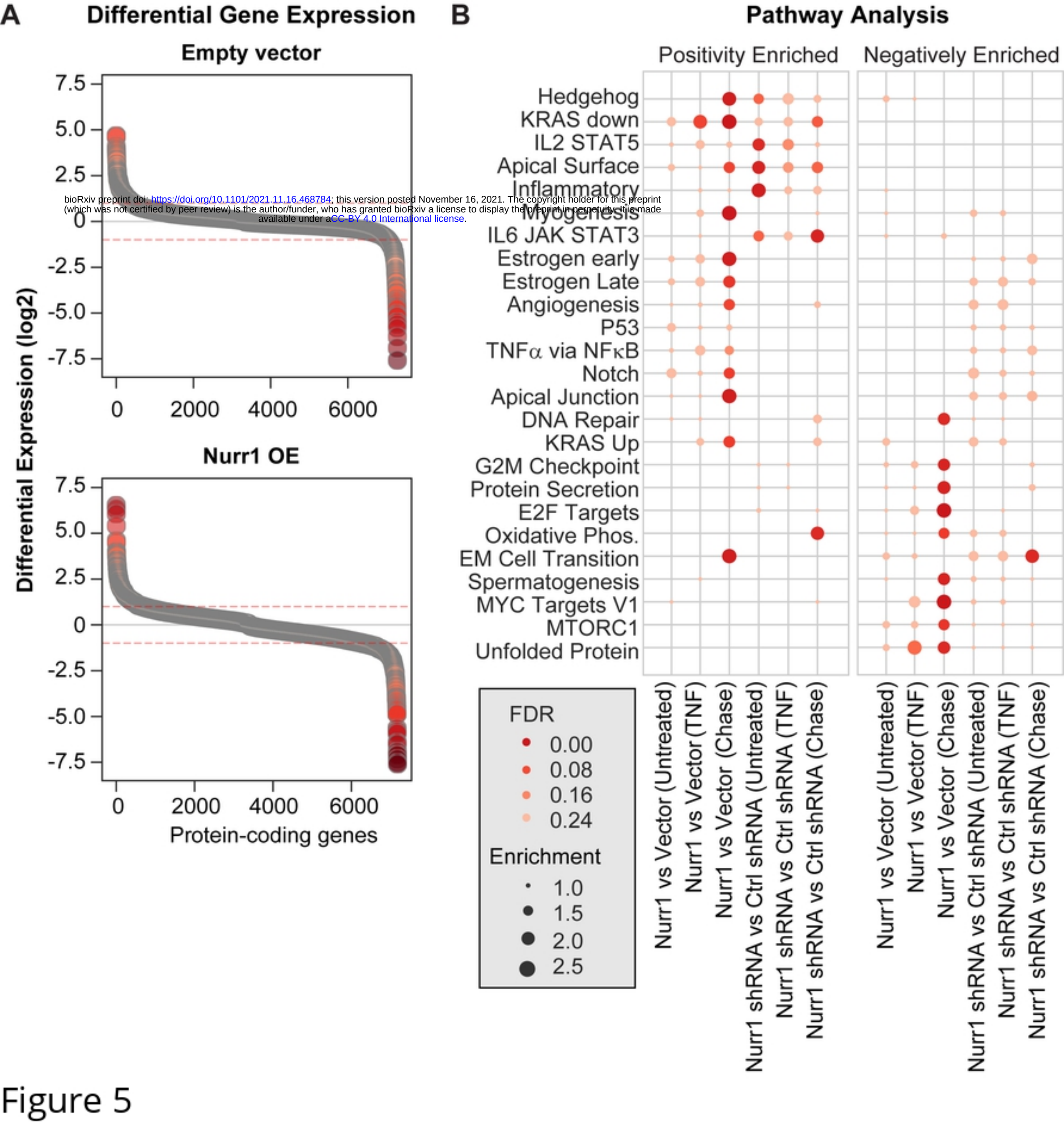

Figure 5

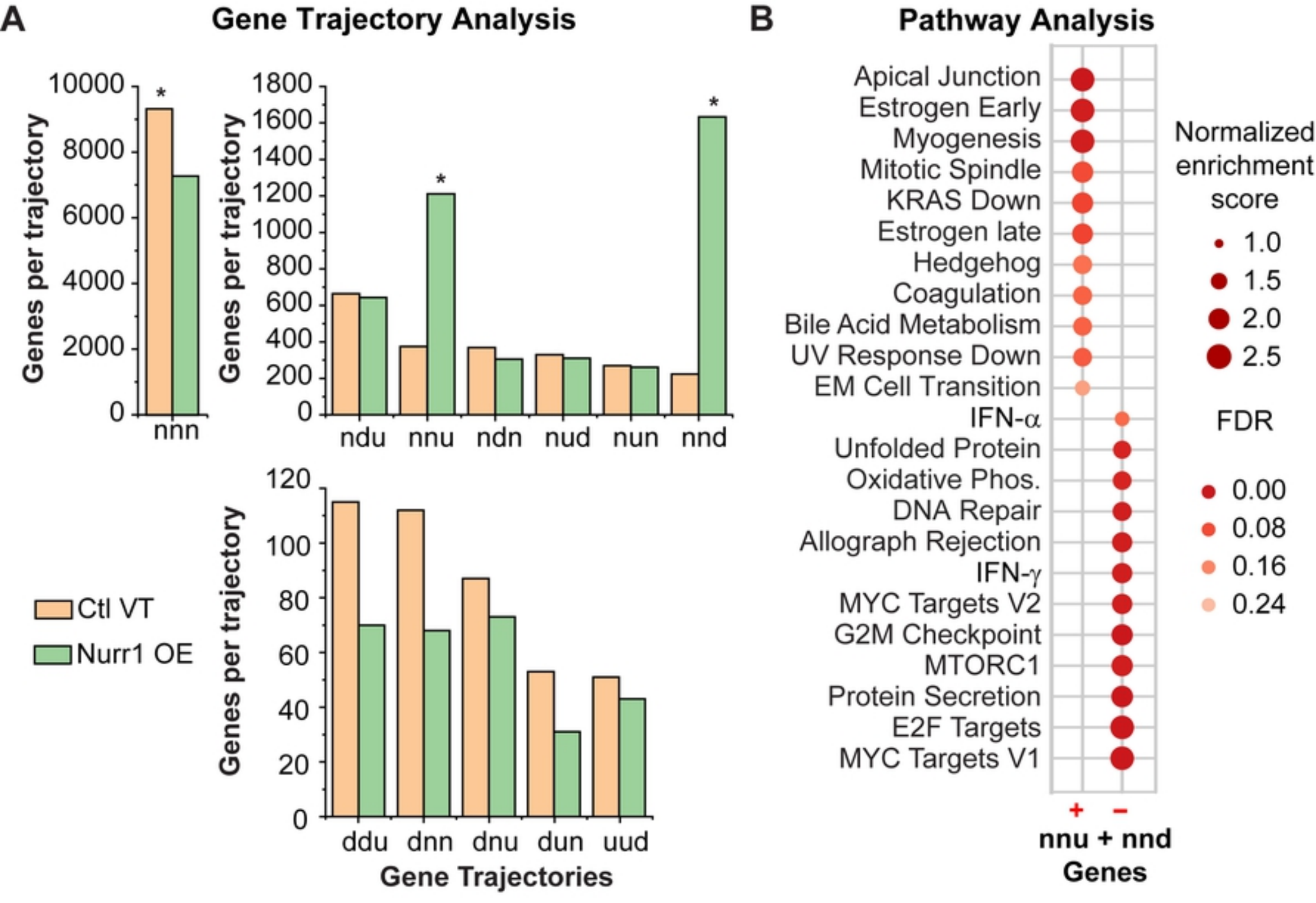
A
Gene Trajectory Analysis
Genes per trajectory
10000
8000
6000
4000
2000
0
*
nnn
1800
1600
1400
1200
1000
800
600
400
200
0
*
*
ndu
nnu
ndn
nud
nun
nnd
120
100
80
60
40
20
0
ddu
dnn
dnu
dun
uud
Gene Trajectories
Ctl VT
Nurr1 OE
B
Pathway Analysis
Apical Junction
Estrogen Early
Myogenesis
Mitotic Spindle
KRAS Down
Estrogen late
Hedgehog
Coagulation
Bile Acid Metabolism
UV Response Down
EM Cell Transition
IFN-α
Unfolded Protein
Oxidative Phos.
DNA Repair
Allograph Rejection
IFN-γ
MYC Targets V2
G2M Checkpoint
MTORC1
Protein Secretion
E2F Targets
MYC Targets V1
+
−
nnu + nnd
Genes
Normalized enrichment score
1.0
1.5
2.0
2.5
FDR
0.00
0.08
0.16
0.24

Figure 6

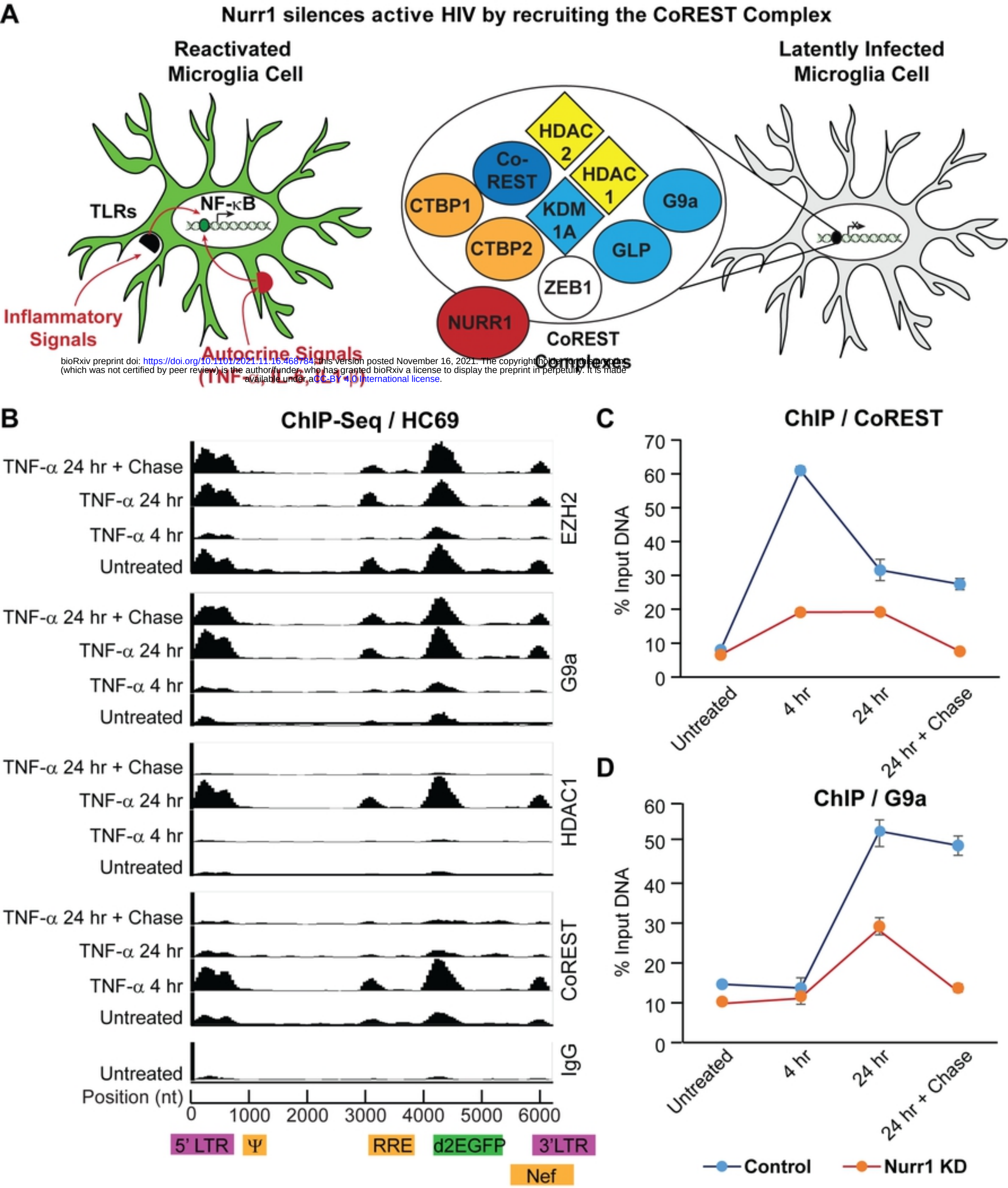

Figure 7

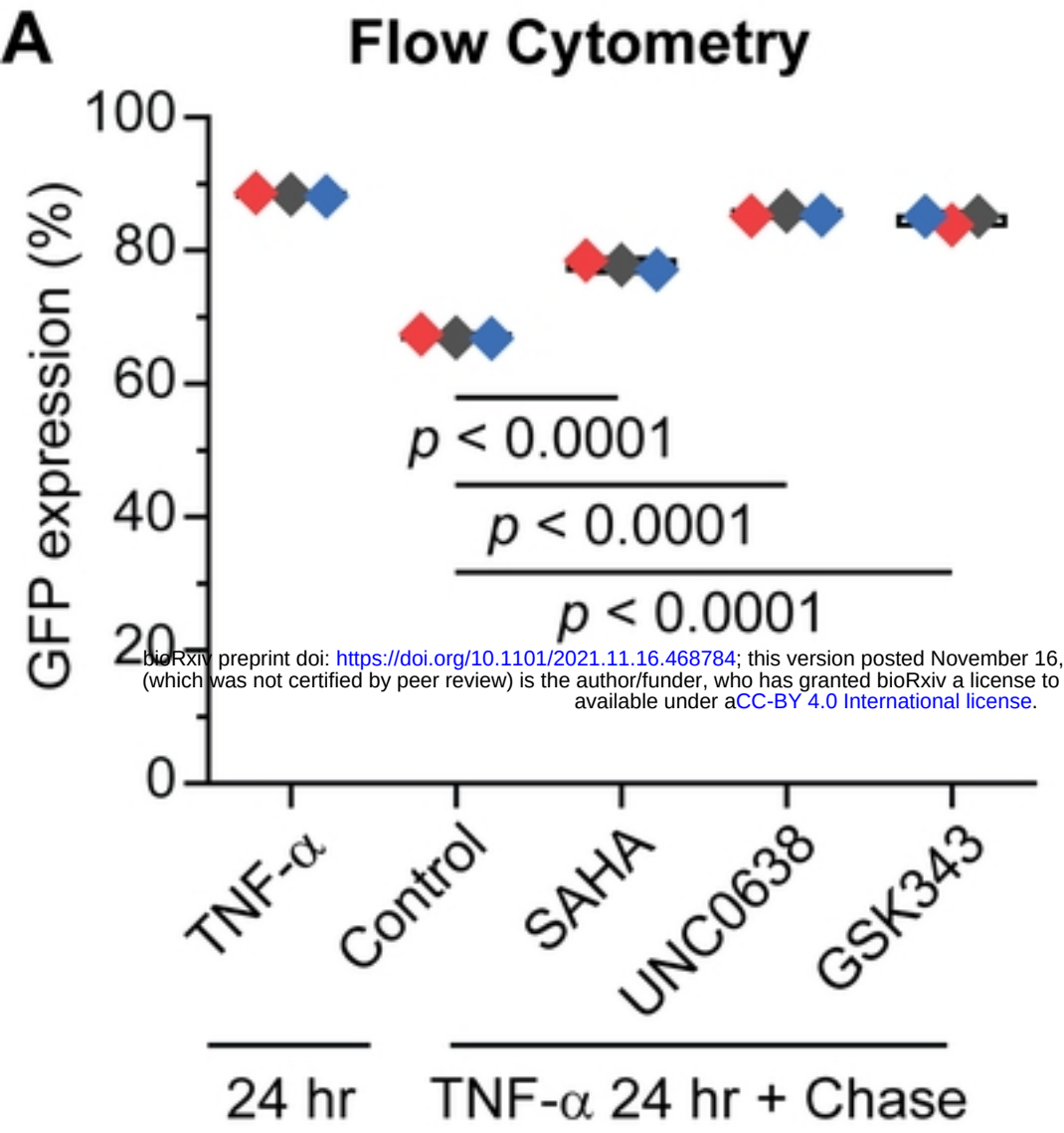

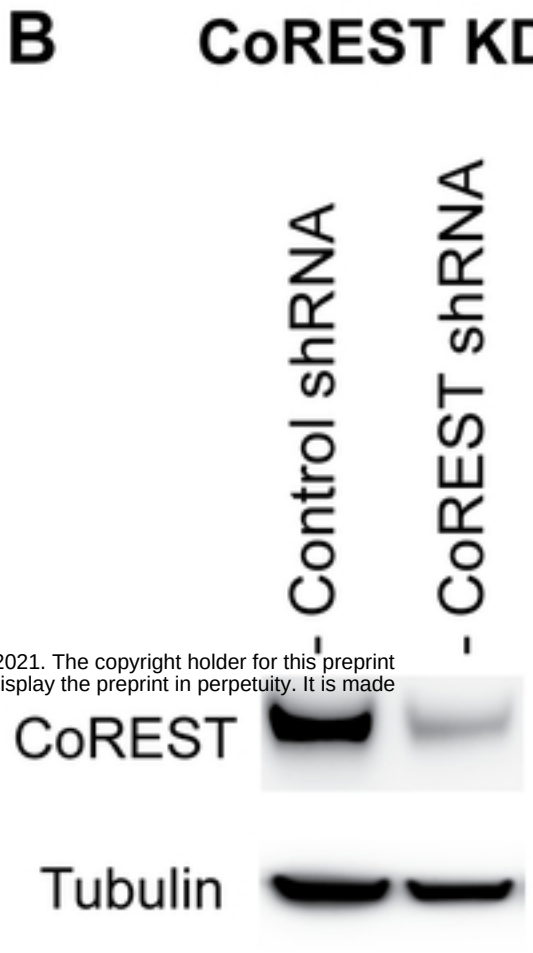

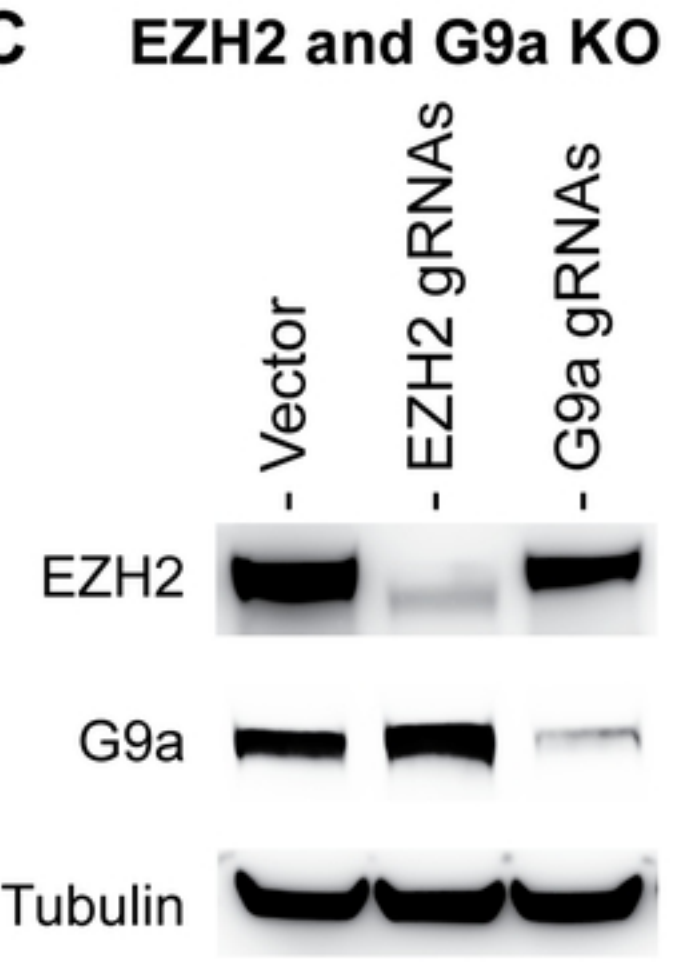

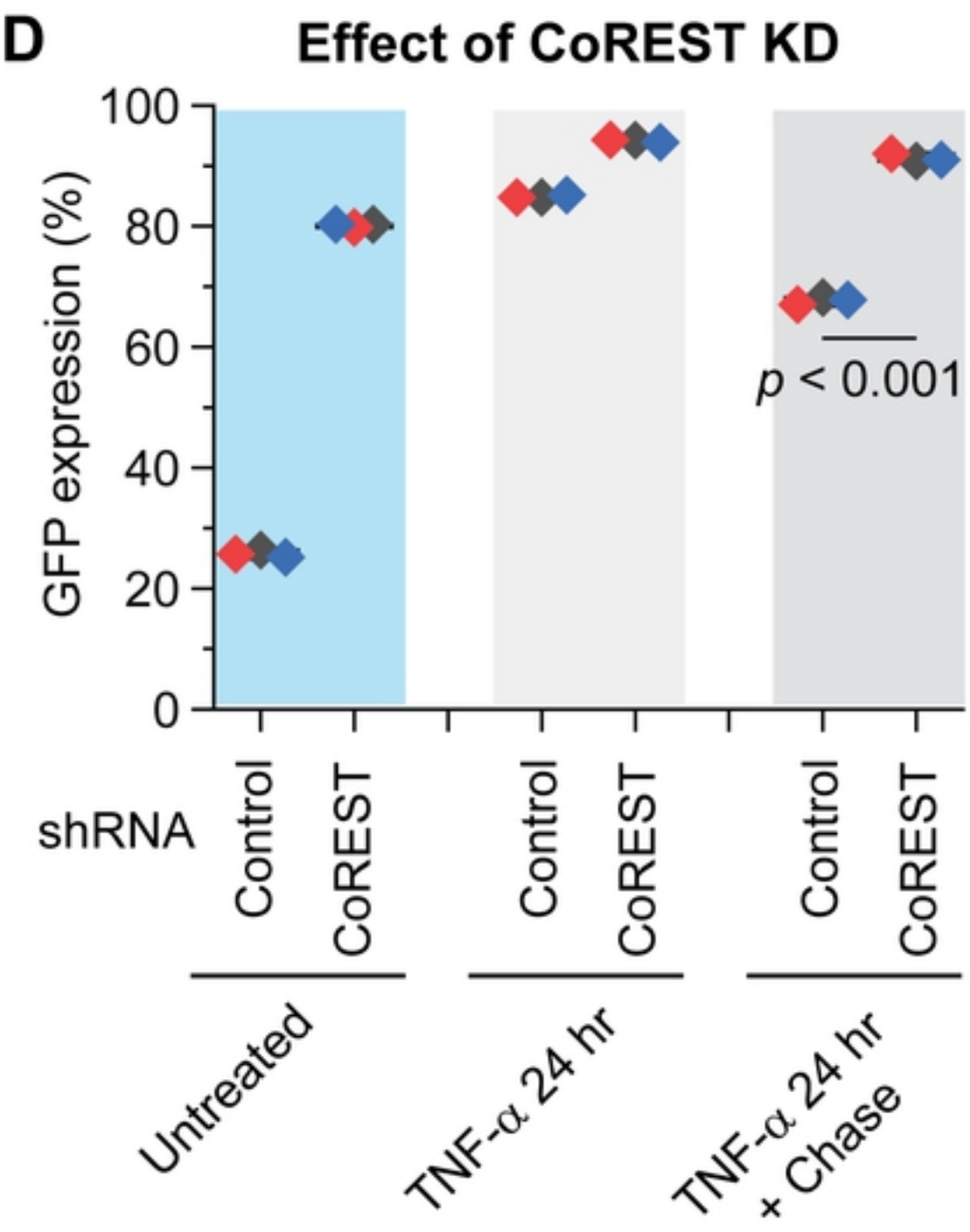

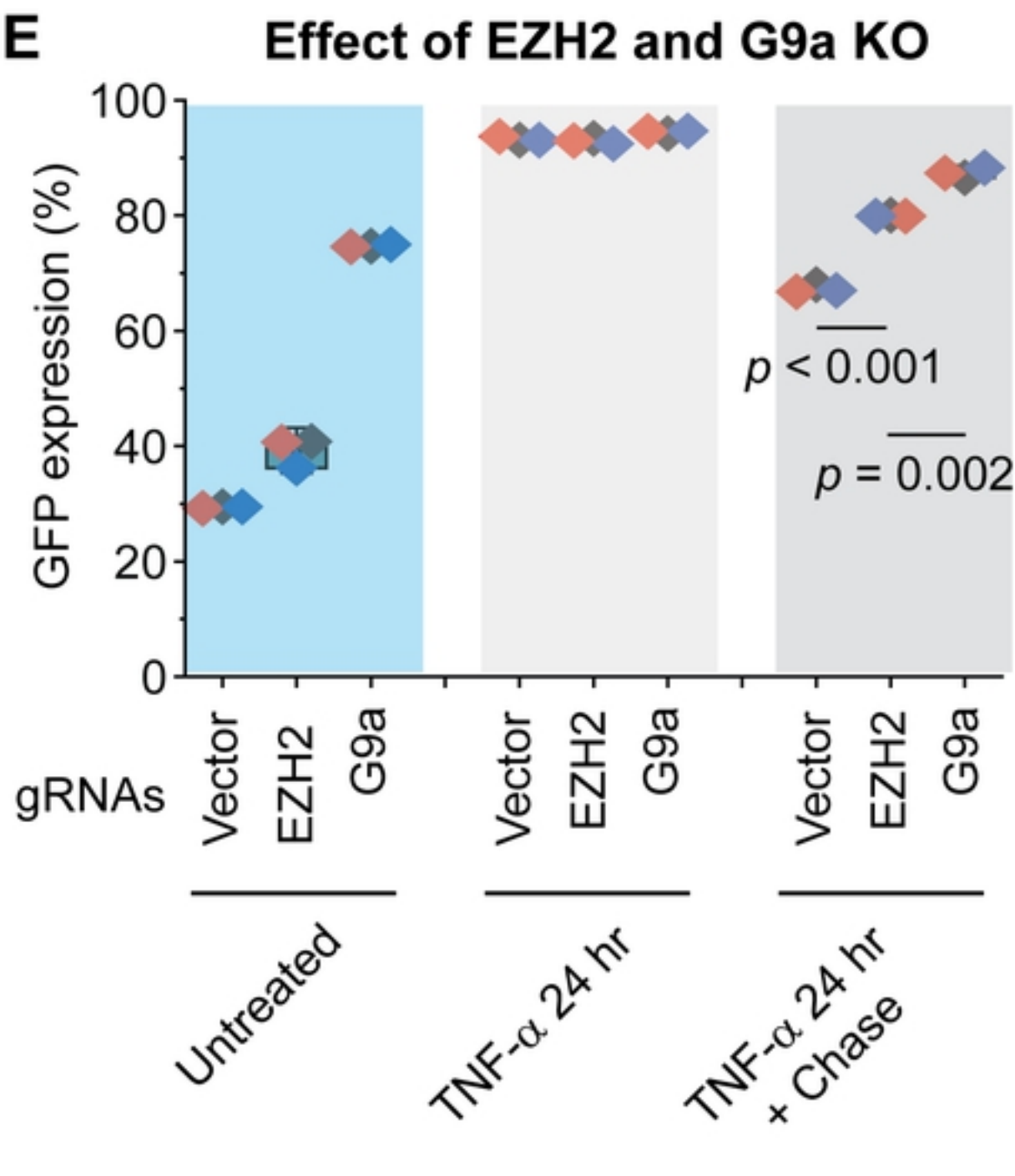

Figure 8

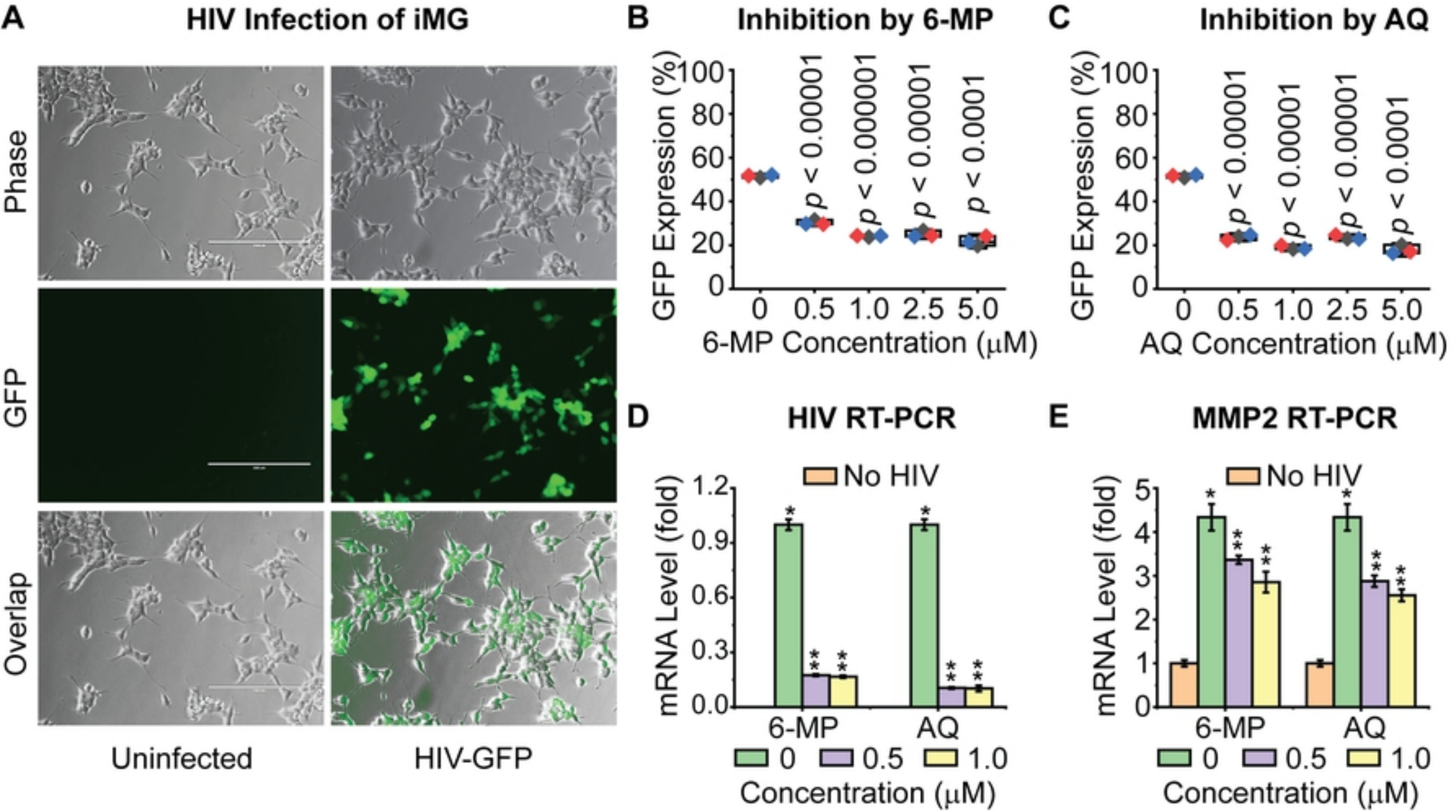
A
HIV Infection of iMG
Phase
GFP
Overlap
Uninfected
HIV-GFP
B
Inhibition by 6-MP
GFP Expression (%)
p < 0.00001
p < 0.000001
p < 0.00001
p < 0.0001
6-MP Concentration (μM)
C
Inhibition by AQ
AQ Concentration (μM)
D
HIV RT-PCR
mRNA Level (fold)
No HIV
6-MP
AQ
Concentration (μM)
E
MMP2 RT-PCR

Figure 9